Vezércikk

Kiss Rita M.
vendégszerkesztő
rita.kiss@mogi.bme.hu

DOI: 10.17489/biohun/2019/1/0h

A Biomechanica Hungarica összes lapszámára jellemző a sokszínűség. Vendégszerkesztőként a szám összeállításakor is e hagyomány folytatására törekedtem. Professzorok, doktoranduszok és témavezetők, orvosok és mérnökök, edzők és mérnökök kutatásait összefoglaló cikkek egy jó kaleidoszkópként nem csak az egyes tudományterületek sokszínűségét, hanem a biomechanika egységes, de egyben sokszínű, mindig a változó igényekhez alkalmazkodó képességét is megmutatják.

A lapszámban összefoglalt egyik kutatás felhívja a figyelmet arra, hogy a pes planus (lúdtalp) hogyan befolyásolja a gerinc alakját, míg egy másik cikk fiatal sportolók esetén a gerinc alakjának és a törzsizomzat aktivitásának változását mutatja be a törzserő tesztek esetén. A 3D nyomtatásnak egyre fontosabb szerepe van az orvostudományban, különösen a protetikában. Két cikk is foglalkozik e témával: a titán alapú 3D nyomtatással előállított egyedi protézisekkel, míg a másik cikk az UHMWPE anyagból 3D nyomtatással elállított protézisek mechanikai tulajdonságait elemzi. A protetika témakörhöz tartozik a tranexamin sav hatásának elemzése a teljes térdízületi protézis beültetés során. Ebben a lapszámban a sporttudományhoz, az ortopédiához köthető kutatások mellett a lapszám egyik cikke az áramlástan alapvető egyenleteit felhasználva a drain-katéterekben történő epeáramlás modellezhetőségét mutatja be.

Tisztelt Olvasó!

Reméljük Ön is megtalálja e lapszámban azokat a magyar és angol nyelvű cikkekben összefoglalt tudományos eredményeket, amelyeket későbbi kutatásaiban fel tud használni!

Jó olvasást kíván:

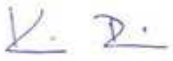

Európai Unió
Európai Regionális Fejlesztési Alap
MAGYARORSZÁG KORMÁNYA
BEFEKTETÉS A JÖVŐBE
SZÉCHENYI 2020

A VARINEX ZRT. ÁLTAL VEZETETT KONZORCIUM

SAJTÓKÖZLEMÉNY

OSTEOINTEGRÁCIÓT LEHETŐVÉ TÉVŐ IMPLANTÁTUMOK KUTATÁSA ÉS TRABEKULÁRIS SZERKEZETEK KIFEJLESZTÉSE ADDITIVE MANUFACTURING ALKALMAZÁSÁVAL

A VARINEX Zrt. K+F versenyképességi és kiválósági együttműködések c. felhívására benyújtott, GINOP-2.2.1-15-2017-00055 azonosítószámmal nyilvántartott támogatási kérelmét a Gazdaságfejlesztési Programok Végrehajtásáért Felelős Helyettes Államtitkárság támogatásra érdemesnek ítélte. A támogatást a VARINEX Zrt. által vezetett konzorcium kapta, amelynek további tagjai: Debreceni Egyetem, Nyíregyházi Egyetem és a Kereken-Pálya Kft.

A pályázat által támogatott kutatás négy éve során lehetőség adódik olyan anyagszerkezet kifejlesztésére, amelyek a jelenleginél magasabb szinten elégítik ki az fémből készült csont- és ízületpótló implantátumokkal szemben jelentkező egyre fokozottabb igényeket. A projektben tervezett állatkísérletek és képfeldolgozási technológiák alkalmazásával célunk a titán alapú fémimplantátumok olyan trabekuláris struktúrájának megalkotása, amely minden eddig ismert megoldásnál jobban biztosítja az osteointegrációt.

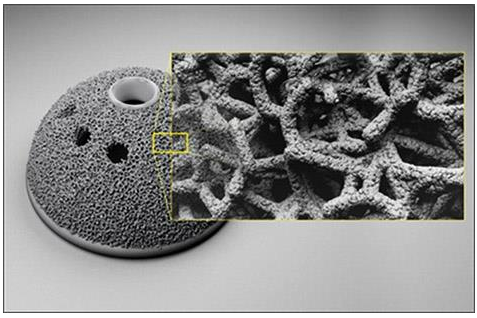

Trabekuláris szerkezetű titán

A projektfeladatok egymásra épülése révén az anyagfejlesztési irányvonalat a projektben részt vevő két egyetem egymással együttműködve alapozza meg, majd az állatkísérletek folyamatosan érkező részeredményei révén közvetlen visszacsatolást valósítunk meg, amely biztosítja a több ciklusú fejlesztési folyamat magas színvonalú végrehajtását és annak nemzetközileg is figyelemre méltó eredményét.
A projekt célja, hogy a jelenleginél lényegesen idő- és költséghatékonyabb módszerekkel, Additive Manufacturing (AM) technológiával állítson elő olyan implantátumokat, melyek az emberi szervezet számára magasabb fokú biokompatibiltást és biofunkcionalitást jelentenek, gyorsabb gyógyulás és jelentősen hosszabb idejű használhatóság mellett. Mindezeken túl további cél, hogy az AM egyes különálló megoldásait teljes körűen áttekintse, összefoglalja a napi sebészi gyakorlathoz szükséges tapasztalatokat, illetve kiegészítse azokat a sebészet igényeinek megfelelően, amely igények jelentős mértékben eltérhetnek az iparban használt és elfogadott AM megoldásoktól.
A csont- és ízületpótló implantátumok alkalmazása területén szeretnénk az AM technológiák adta lehetőségeket többek között képfeldolgozási algoritmusokkal és állatkísérletekkel vizsgálni, és gyakorló sebészekkel közösen kidolgozni az egyes felmerülő feladatok megoldását oly módon, hogy a keletkező tudás minden csont- és ízületi implantátummal foglalkozó személy, szervezet számára egyetemesen elérhető legyen.

Projekt megvalósítási időtartama: 2017.08.01. - 2021.07.31.

Projekt összköltségvetése: 2.000.000.000 Ft
Támogatás összege: 1.670.000.000 Ft

Sajtókapcsolat: Falk György, Tel.: +36 309-526-528, E-mail: falk@varinex.hu

THE ELEMENTS OF FLUID MECHANICS OF BILE FLOW THROUGH BILIARY DRAINAGE CATHETERS

Wenguang Li

School of Energy and Power Engineering, Lanzhou University of Technology

liwg40@sina.com

DOI: 10.17489/biohun/2019/1/03

Abstract

Obstructive jaundice in the biliary tract can infect blood and result in mortality with a high rate. Percutaneous transhepatic biliary drainage (PTBD) with catheters is a useful solution discharging the obstructive jaundice. However, the elements of fluid mechanics showing clinical performance of a PTBD catheter have been documented little so far. In the article, empirical relationships between bile flow rate and pressure gradient in PTBD catheters were studied in terms of equivalent friction factor for the first time. Firstly, an equivalent friction factor in a catheter was raised and determined based on existing in vitro experimental data of bile flow through the catheters with different materials, various inner diameters and lengths under various pressure differences. Then, an empirical correlation of bile flow rate through a catheter was established based on pressure gradient, inner diameter and bile viscosity. The correlation was used to identify effects of catheter inner diameter and bile viscosity on the bile flow rate under the physiological bile pressure difference across obstructed common bile ducts. The feature of minor hydraulic losses in the catheters was clarified, too. The proposed equivalent friction factor was proportional to Reynolds number in a power of -0.654 in comparison with a power of -1 for the fully developed laminar flow in circular pipes. The bile flow rate through a catheter was proportional to inner diameter, kinematic viscosity, and pressure gradient in the powers of 3.2, -0.5 and 0.74, respectively. The minor hydraulic losses could be significant when Reynolds number was greater than 100.

Keywords: percutaneous transhepatic biliary drainage; biliary drainage catheter; bile; flow rate; friction factor; Reynolds number

Introduction

Obstructive jaundice is a special situation of jaundice when the bile is stopped flowing into the duodenum and remains in the blood due to gallstones in the common bile duct or extrinsic compression by tumours external to the common bile duct. The obstructive jaundice is a serious condition associated with high mortality rates and should be treated instantly by using percutaneous transhepatic biliary drainage (PTBD). PTBD is a procedure based on which the blocked bile is discharged into a drainage bag outside of the human body (external drainage in *Figure 1a*) or the duodenum through the common bile duct (internal drainage in *Figure 1b*) by using a catheter.[1,2] The internal drainage, the bile can flow in the internal catheter or flow into the bag thorough the external drainage catheter, depending on the resistance in the two catheters.

Even though PTBD is palliative, but it can improve quality of life for patients with benign and malignant biliary diseases with success rates of 82-99 %.[3-11] PTBD has been become an effective method for relief of biliary obstruction associated

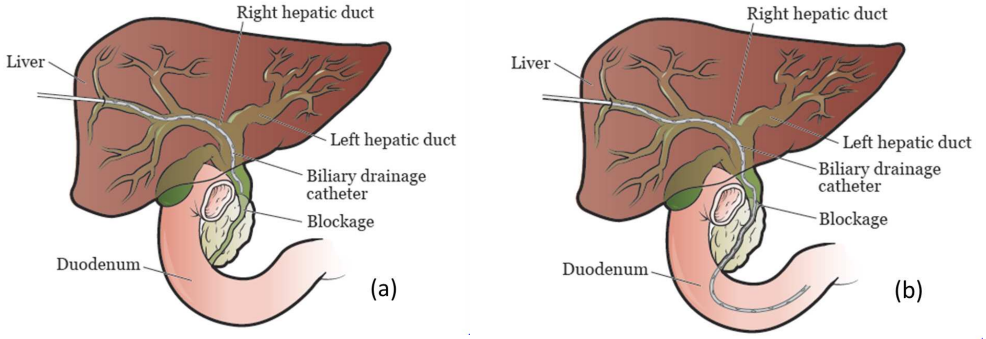

Figure 1. The external (a) and internal (b) percutaneous transhepatic biliary drainage, the pictures are from https://www.mskcc.org/cancer-care/patient-education/about-your-biliary-drainage-catheter

with both benign and malignant conditions.

Even though PTBD in patients is replaced every 4 or 6 weeks, unfortunately, PTBD is subject to complications after patients with malignant biliary disease undergo placement of drainage catheter.[6-8, 10, 12, 13] The complications can be cholangitis, catheter dislodgement, leaking around catheter, obstructed catheter, hemobilia, hypersecretion of bile, bilio-pleural fistula, bile duct perforation and pneumothorax[14], their occurrence percentages in 179 patients are illustrated in *Figure 2*. The total percentage of the complications related to catheter is as high as 43%. This means that the catheter performance plays a vitally important role in PTBD technique.

The catheter dislodgement and leaking complications connect with catheter design and soft tissue bimechanical property, while the catheter obstruction is associated with catheter design and bile fluid mechanics inside. Even though the catheter obstruction has made a 12.3% contribution to the total complication occurrence, it can cause catheter malfunction

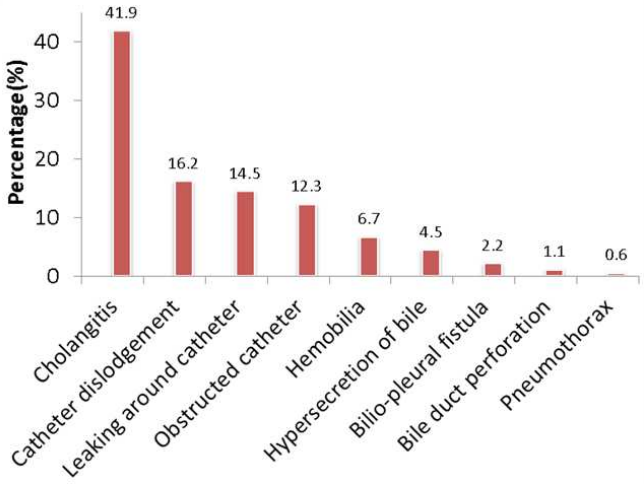

Figure 2. The percentages of complications after PTBD occurred in 179 patients with malignant biliary obstruction, the percentages were recalculated based on the data in the table in[14]

Material	D (French)	d (mm)	L (cm)	Flow rate Q(ml/s) under a pressure difference (cmH_2O)			
				1	2	6	9
Polyethylene	6.3	1.4	65	0.023	0.056	0.088	0.153
	7.1	1.5	65	0.028	0.068	0.110	0.165
	8.3	1.8	50	0.114	0.184	0.296	0.428
	10	2.2	50	0.210	0.385	0.495	0.701
Polyurethane	10	2.0	50	0.094	0.182	0.300	0.450
	12	2.7	50	0.256	0.456	0.769	1.110
Polyvinyl-chloride(PVC)	10	2.2	60	0.111	0.250	0.410	0.620
	10	2.2	50	0.153	0.333	0.500	0.800
Silicon elastomer	16	2.8	65	0.294	0.549	0.694	1.000
	16	2.8	50	0.310	0.595	0.833	1.330
Teflon	12	3.0	65	0.303	0.400	0.690	0.952
		3.0	31	1.300	1.540	2.000	2.500

Table 1. Measured flow rates through selected drainage catheters under specified pressure differences Effective length of catheter is the distance from catheter hub to first side hole, 1 French=1/3 mm

and eventually result in PTBD failure. From this point of view, attention should paid to design and fluid mechanics of catheter in PTBD.

Presently, investigations into design and fluid mechanis of catheter in PTBD are lack. Kerlan et al,[15] in the first time, measured bile flow rates through a series of different catheters at various pressure differences across the catheters in vitro, but their raw data remained unprocessed. Bret et al,[16] clinically applied large size silicone catheters with 12, 15, 18 French outer diameters (1 mm=3 French), 2, 3, 4 mm inner diameters and 3×5, 4×7, 5 mm×9 mm side holes into 30 patients with obstructive jaundice due to stenoses and tumours in bile ducts for a long-term. It was shown that PTBD was effective in treating benign and mailignant bile duct strictures for a long-term, but frequently minor problems, mostly catheter-related, did persist.[17]

A few in vitro experiments on fluid flow in percutaneous drainage catheters have been made by measuring drainage time at various catheter sizes and fluid viscosities.[18] It was demonstared that a more viscous fluid required more large catheter to secure a rapid drainage. The flow rates of commerical multipurpose pigtail drainage catheters were measured in vitro at 30 mmHg presssure difference. Since their inner diamter sizes were compariable, their flow rates were simliar in values.[19] The effects of number and location of drainage catheter side holes on liquid flow rate were measured in vitro by emplying unilateral and bilateral side hole models, the catheters with bilateal side holes had a higer flow rate than those with unilateral side holes, adding more side holes could not improve flow rate once the number of the holes beyond a critical number of holes.[20]

The flow rates of simulated bile such as water, three additional water solutions of guar gum (four dynamic viscosities) through three kinds of pigtail cathetes (two multipurpose drainage catheters, one bilary drainage catherter) were measured in vitro at 12 cmH_2O pressure difference under side hole unobstructed and

Catheter		Bile			
d (mm)	L (cm)	ρ (kg/m3)	μ (Poise)	ν (mm^2/s)	Δp (cmH_2O)
1.4	50	1000	0.01, 0.02	1, 2	11.8-18.4
1.8	50	1000	0.01, 0.02	1, 2	11.8-18.4
2.2	50	1000	0.01, 0.02	1, 2	11.8-18.4
2.7	50	1000	0.01, 0.02	1, 2	11.8-18.4

Table 2. The known parameters for a clinical application

obstructed conditions, and it was identified that the number of side holes did not affect in vitro biliary catheter drainage.[21] The influence of catheter connections of catheter drainage flow rate was identified in vitro experimentally, it was shown that flow rates could be decreased significantly by connections, especailly when the inner diamater of a connection was smaller than the inner diameter of the catheters connected.[22]

A method was proposed to predict the clogging effect drainage catheters based on in vivo rabbit experiments by monitoring intra-catheter pressure.[23] The commerical catheter for PTBD was ligated with a nylon thread just proximal to the first side hole to pervent the catheter obstruction caused from jejunobiliary reflux of the intestinal contents in internal PTBD.[24] Fracture of the PTBD catheter could occure and cause bile peritonitis.[25] Three new techniques were developed to retrieve fractured and intrahepatically dislodged PTBD catheters.[26]

Based on existing results on PTBD catheters mentioned above, bile fluid mechanics associated with clinical performance of catheters has been documented a little so far, and there are no empirical relationships for bile flow through biliary drainage catheters to assess their clinical performance in the literature currently. In the paper, the raw experimental data of a series of catheters on bile flow rate and pressure difference were analysed based on the elements of fluid mechanics to make the dead experimental data alive. An equivalent friction factor through the catheters was proposed and determined by using these observed data. An empirical relationship of bile flow rate through a catheter was estabilshed accordingly and applied to predict the bile flow rates through the catheters with various inner diameters under measured normal and abnormal biliary pressures and two bile viscosities in a common bile duct. The effects of catheter inner diameter and bile viscosity were clarified. The work can be meaningful to catheter fluid mechanics in biomedical/biomechanical engineering and clinical practice in PTBD procedure.

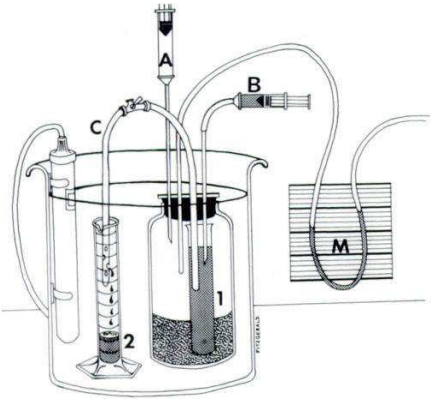

Figure 3. The experimental set-up for bile flow measurement through catheter in Kerlan et al.[15] A bile stream is established in the catheter segment C by the pressure difference from chamber 1 to chamber 2 when the bile is at 37°C temperature

Experimental data

Catheters for PTBD are a flexile, plastic central-hollowed tube with taping head and side holes as shown *Figure 3a*. In vitro bile flow meansuremts through the catheters have been very rare in the literature so far. At the moment, just one relatively complete data set for such flow measurement was identified in Kerlan et al.[15] The experimental set-up in the mesurements is illustarted in *Figure 3b*. A catheter (C) connects chamber 1 and chamber 2. Chamber 1 is pressurised and depressurised by adding and removing air with syringe A to maintain a constant pressure difference across the catheter and estabilsh a bile flow in it. This pressure difference is measured by using U-tube manometer (M). Bile level is held to be contant with syringe A by infusing bile. All chambers are submerged in a water bath to allow bile temperautre to be at 37 °C.

Freshly aspirated human hepatic bile with a dynamic viscosity of 0.01 Poise (0.001 Pa·s) and a density of 1000 kg/m^3 serves as experimental fluid.[15] The experimental pressure differences, catheter sample lengths and diameters and measured bile flow rates are listed in *Table 1*.[15]

These raw exprimental data are going to be utilised to estabilish an empirical relationship between flow resistance factor/equivalent friction factor and Reynolds number and a correlation between bile flow rate and pressure gradient.

Empirical relationships

Equivalent friction factor

The hydraulic losses in the catheter shown in *Figure 3b* include the friction loss over the wet surface, the incidence loss at the inlet of catheter, the secondary flow loss in the 180° bend, and the diffusion loss across the side holes. At first, these losses are supposed to contribute an equivalent friction factor to simplify the problem; then, according to the skin friction factor formula for ducts,[27] the equivalent friction factor will be calculated based on a known pressure difference, bile flow rate, effective length of the catheter and inner diameter of the catheter in the following manner

$$\lambda = \frac{\Delta p}{\frac{V^2}{2g}\frac{L}{d}} \qquad (1)$$

where is the gravity acceleration, g = 9.81 m/s^2, V is the mean bile flow velocity. Because of $V = Q/\left(\pi d^2/4\right)$ [27], *Eq. (1)* can be rewritten as

$$\lambda = \frac{g\pi^2 d^5}{8Q^2}\frac{\Delta p}{L} \qquad (2)$$

As a result, the corresponding λ - Re scattered data points based on the experimental data in *Table 1* is present in *Figure 4*, where

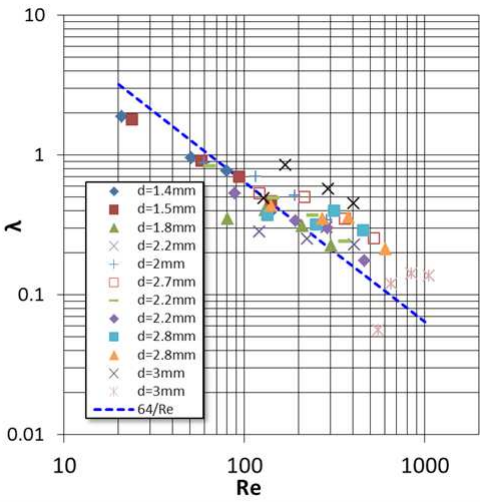

Figure 4. The scattered equivalent friction factors based on the experimental data in *Table 1* and the analytical friction factor are plotted as a function Reynolds number

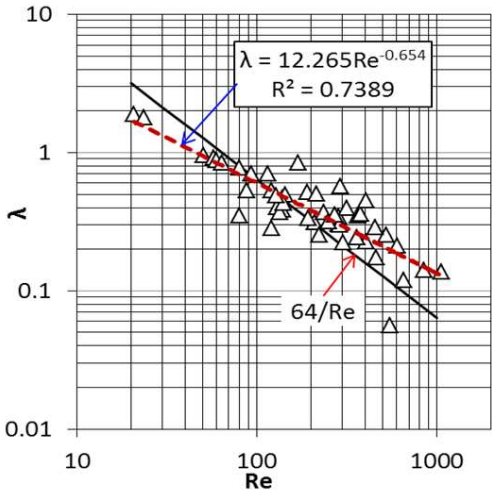

Figure 5. The fitted empirical correlation of equivalent friction factor in terms of Reynolds number and its comparison with the analytical friction factor for a catheter, the scattered data points are the same as those in *Figure 4*, the inner diameter is no longer indicated

$\mathrm{Re} = 4Q/\pi d\nu$, is the bile kinematic viscosity, ν = 1 mm^2/s.[15] Because of $\mathrm{Re} \leq 1000$, the bile flow in the experimental catheters was in laminar regime. For comparison, the analytical friction factor for the fully developed laminar flow in a circular pipe in[27] is plotted, too.

In the figure, some experimental points are below the $64/\mathrm{Re}$ curve as $\mathrm{Re} \leq 200$, and some points are above the curve, suggesting the experimental shares a different slope with the analytical friction factor curve. The experimental has been best fitted by a power function of , the empirical formula is read as

$$\lambda = \frac{12.265}{\mathrm{Re}^{0.6540}}, \quad R^2 = 0.7389 \qquad (3)$$

where is the correlation coefficient. A comparison of the experimental with the fitted curve is made in *Figure 5*.

The relationship of bile flow rate to pressure gradient

An empirical correlation for λ has been established by *Eq. (3)* based on fluid mechanics method, the λ expression is involved into *Eq. (2)*, and following equation is achieved

$$\frac{12.265}{\mathrm{Re}^{0.6540}} = \frac{g\pi^2 d^5}{8Q^2}\frac{\Delta p}{L} \qquad (4)$$

Putting the Reynolds number $\mathrm{Re} = 4Q/\pi d\nu$ into *Eq. (4)*, and the following equation is established

$$\frac{12.265}{\left(\frac{4Q}{\pi d\nu}\right)^{0.6540}} = \frac{g\pi^2 d^5}{8Q^2}\left(\frac{\Delta p}{L}\right) \qquad (5)$$

From *Eq. (5)*, the bile flow rate through a catheter with the length driven by a pressure gradient can be solved and expressed by

$$Q = \frac{8.3186 g^{0.7429}\pi d^{3.2288}}{128\nu^{0.4859}}\left(\frac{\Delta p}{L}\right)^{0.74} \qquad (6)$$

where the units of Q, d, L, Δp and ν are m^3/s, m, m, mH2O, kg/m^3, m^2/s, respectively. In the equation, $Q \propto d^{3.2}\ \nu^{-0.49}\left(\Delta p/L\right)^{0.74}$ is held approximately.

For the fully developed laminar flow in a catheter, the friction factor is expressed analytically by $\lambda = 64/\mathrm{Re}$.[27] Involving the Reynolds number $\mathrm{Re} = 4Q/\pi d\nu$ into *Eq. (2)*, an analytical relationship between bile flow rate and pressure gradient is worked out

$$\frac{12.265}{\mathrm{Re}^{0.6540}} = \frac{g\pi^2 d^5}{8Q^2}\frac{\Delta p}{L} \qquad (7)$$

where the dynamic viscosity μ is related to the kinematic viscosity with $\mu = \rho\nu$, ρ is the bile density, the unit of Δp is mH_2O. In these

expressions, $Q \propto d^4\ \nu^{-1}\left(\Delta p/L\right)^1$, suggesting parameters d, ν and $\Delta p/L$ exhibit a stronger effect on Q in comparison with those in *Eq. (6)* originated from experimental observations.

Another sort of relation between bile flow rate and pressure gradient

In the relationship of bile flow rate to pressure gradient section, an empirical friction factor is determined first, then it replaces the λ in *Eq. (2)*, and Re is experienced in terms of bile rate; finally, a relationship between bile flow rate and pressure gradient is sought as expressed with *Eq. (6)*. In fact, we can derive an empirical relationship between bile flow rate and pressure gradient directly based on analytical *Eq. (7)*. This method has used in the determination of an empirical expression between bile flow rate and pressure gradient across animal biliary tree in vitro in.[28] This method will be tried on the experimental data on the catheters[15] here.

A few perfusion experiments were performed on the biliary tree (hepatic, cystic and common bile ducts) of six fasting mongrel dogs[28] by using saline and bovine bile at different bile perfusion flow rates, respectively. The pressure differences across the tree were recorded. It was identified that the experimental scattered points of ($\Delta p/L$,) and ($\rho g\Delta p/L$, $128\mu Q/\pi d^4$) can be best fitted with a linear relationship in a log-log plot. Then the bile flow rate can be obtained in terms of pressure gradient, like *Eq. (7)*.

In doing so, the experimental data points of $\Delta p/L$ -$128\nu Q/\pi g d^4$ and $\rho g\Delta p/L$ -are plotted and fitted, respectively, for the experimental data in the catheters in [15]. The experimental scattered data points and the corresponding regression formulas are illustrated in *Figure 6*. Based on these formulas, the bile flow rate through a catheter under a known pressure gradient is given by

$$Q = \frac{0.3234\pi g d^4}{128\nu}\left(\frac{\Delta p}{L}\right)^{0.6458} \quad \text{or}$$

$$Q = \frac{8.573\pi d^4}{128\mu}\left(\frac{\rho g\Delta p}{L}\right)^{0.6458},\ R^2 = 0.7487 \quad (8)$$

where the units of Q, d, L, Δp, ρ, ν and μ are m3/s, m, m, mH2O, kg/m3, m2/s, Pa.s, respectively.

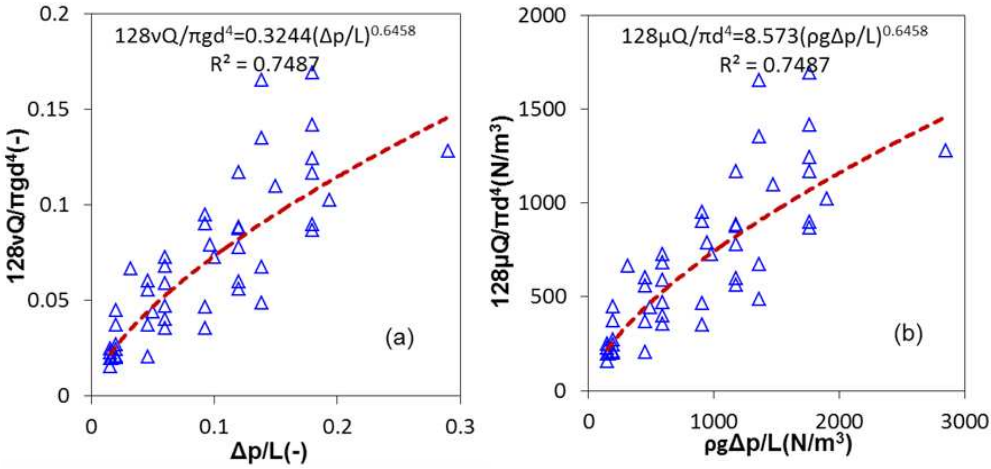

Figure 6. The scattered data points of ($\Delta p/L$, $128\nu Q/\pi g d^4$) and ($\rho g\Delta p/L$, $128\mu Q/\pi d^4$) as well as the corresponding regression formulas, the scattered data points are the same as those in *Figure 4*, the inner diameter is no longer indicated

A comparison of two kinds of relationship

From the same set of experimental data, two relationships have been obtained for bile flow rate in terms of pressure gradient across a catheter expressed by *Eq. (6)* and *(8)*. Two relationships may result in a different bile flow rate under the same clinical condition. To confirm this effect, a computational example is provided here.

The biliary mean resting pressure in normal human common bile duct is 11.8 cmH_2O, but in the duct with obstructive jaundice, it is 18.4 cmH_2O.[29,30] It is assumed that a 50 cm long catheter is connected to a common bile duct with obstructive jaundice at the 18.4 cmH_2O initial pressure, after drainage persists for a certain long of time, the biliary pressure restores to the normal level of 11.8 cmH_2O. This means that the pressure difference across the

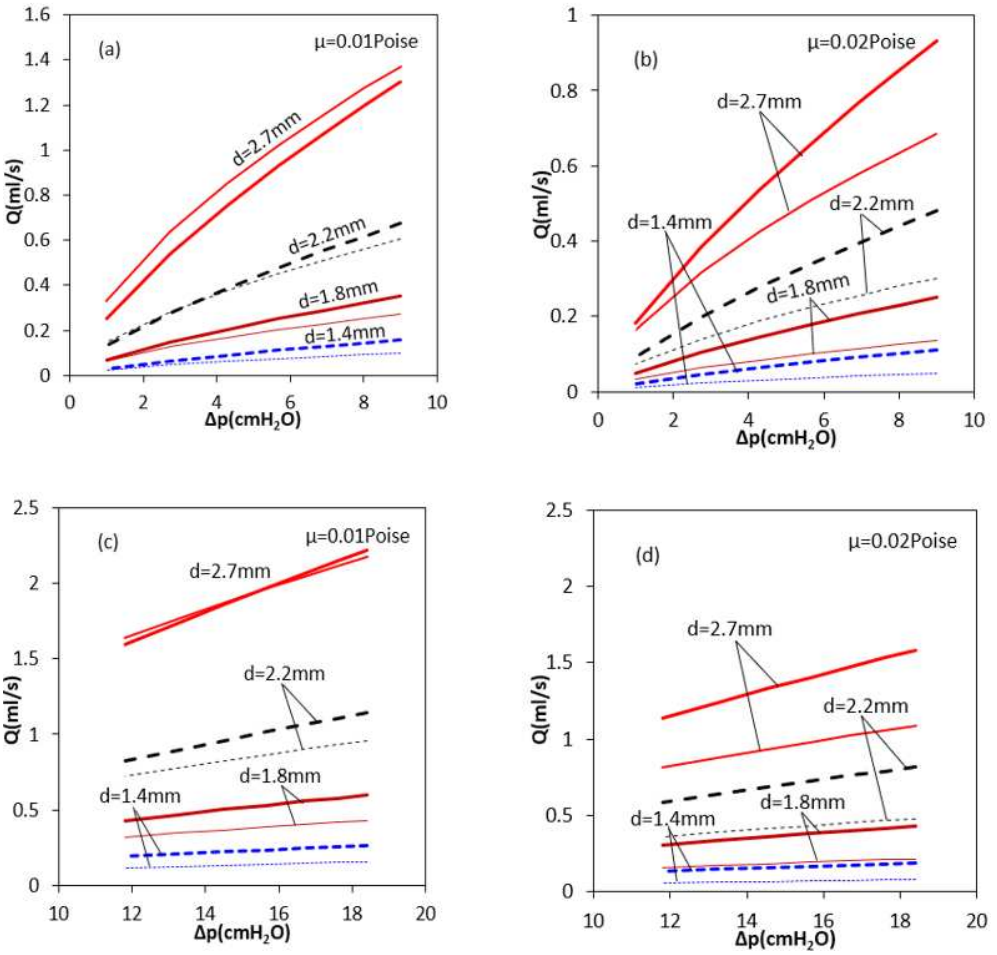

Figure 7. The predicted bile flow rate through four catheters in terms of bile pressure difference across the catheters at two viscosities, the thick lines are for *Eq. (6)*, but the thin lines for *Eq. (8)*; in (*a*) and (*b*), the pressure difference is the range of the experiments in *Table 1*; while in (*c*) and (*d*), the pressure difference is based on clinical observation[29, 30]

catheter varies to 11.8 cmH_2O from 18.4 cmH_2O. The bile dynamic viscosity is 0.01 Poise 15 and 0.02 Poise 31 with a density of 1000 kg/m3. The catheter inner diameters are d =1.4, 1.8, 2.2 and 2.7 mm, respectively, based on *Table 1*. These known parameters are summarised in *Table 2*.

Firstly, *Eq. (6) and (8)* are used to predict the bile flow rates under the experimental conditions such as 1, 2, 6 9 cmH_2O pressure differences and 0.01 Poise viscosity as shown in *Table 1* and at four inner diameters in *Table 2*. The two equations result in nearly the same bile flow rate profiles as shown in *Figure 7a*. This is not surprised because they have originated from the same experimental data set and applied under nearly the same condition in terms of pressure difference, viscosity and catheter inner diameter as in the experiments.[15]

Secondly, two equations are employed to estimate the bile flow rates at 0.02 Poise viscosity, while the rest condition remain the same as those for *Figure 7a*. In the experiments of[15] the tested liquid viscosity was kept being 0.01 Poise. The prediction at 0.02 Poise viscosity is an extrapolation from the results at 0.01 Poise viscosity. The flow rates from Eq. (6) are larger than those from *Eq. (8)*, as demonstrated in Figure 7b because of $Q \propto \nu^{-0.49}$ in *Eq.(6)* rather than $Q \propto \nu^{-1}$ in *Eq. (8)*. These suggest that the flow rates predicted with two equations at a viscosity more than 0.01 Poise are not accurate as those at 0.01 Poise.

Finally, two equations are utilized to calculate Q - Δp curves at four inner diameters and two viscosities in *Table 2* and under the pressure differences higher than those in *Table 1*. The predicted Q - Δp curves are illustrated in *Figure 7c* and *d*. These predictions are extrapolation from an experimental pressure difference in[15] to a higher-pressure difference in clinical observation. Once again two equations lead to a very similar flow rate curve at to 0.01 Poise viscosity, but a very different curve at 0.02 Poise viscosity.

Clearly, the bile flow rate rises with both increasing pressure difference and inner diameter but reduces with increasing viscosity. The effect of inner diameter on the flow rate is the most significant in comparison with that of the other factors. To secure a relatively high bile flow rate and better drainage, a catheter should prefer an inner diameter as big as possible, especially for thick bile.

From *Figure 7c* and *d*, since the bile flow rate is inversely proportional to the viscosity in *Eq. (8)*, the viscosity in *Eq. (8)* exhibits a stronger effect on the flow rate than the viscosity does in *Eq. (6)*. As a result, the flow rates predicted with *Eq. (8)* are smaller than those with *Eq. (6)* in most cases. In the case of d =2.7 mm and μ =0.01 Poise, two equations result in nearly the same flow rate. This is because of the dominated effect of inner diameter on the flow rate.

In the experiments in [15], the fluid viscosity was kept constant. Thus, there is no effect of fluid viscosity reflected both *Eq. (6)* and *(8)*. If the viscosity varied in the experiments in,[15] *Eq. (6)* and *(8)* should lead to a nearly identical bile flow under the same clinical condition. To validate two empirical relationships of *Eq. (6)* and *(8)*, more experimental data on in vitro bile flow measurements in catheters are desirable with more viscous liquids and under pressure differences higher than 9 cmH_2O.

Discussions

In the paper, a set of raw experimental data on in vitro bile flow through a series of catheter samples in[15] was analysed in fluid mechanics context. An empirical equivalent friction factor was figured out and the corresponding flow rate formula of bile through a catheter was

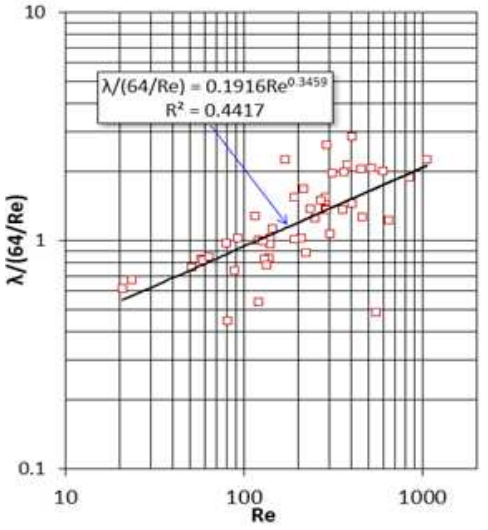

Figure 8. The ratio of the equivalent friction factor to the theoretical friction factor of the fully developed laminar flow in a circular pipe, i.e. as a function of Reynolds number, the scattered data points are the same as those in *Figure 4*, the inner diameter is no longer indicated.

established. Finally, an application example was demonstrated and the effects of catheter inner diameter, pressure difference and bile viscosity were clarified. Such a study has not been found in literature so far. The study in the paper has contributed to the elements of fluid mechanics of catheter in PTBD.

In the equivalent friction factor, there are minor hydraulic losses, namely entry loss at the catheter inlet, secondary flow loss in the bend of a catheter, and diffusion loss through the side holes in the catheter. It is not easily to measure and estimate these minor losses. Here using the ratio of the equivalent friction factor to the theoretical friction factor for the fully developed laminar flow in a circular pipe, i.e. $\lambda/(64/\mathrm{Re})$ is used to estimate these minor losses. As a result, the scattered data points and a regression equation are illustrated in *Figure 8*. Clearly, ratio augments with increasing Re, particularly, if $\mathrm{Re}>100$, then $\lambda/(64/\mathrm{Re})>1$, indicating the dominant minor losses. When $\mathrm{Re}<100$, the ratio is less than one. This effect may be due to some errors in the experiments or the thickening effect of non-Newtonian bile at low flow rate.

Note that, in clinical practice, the bile flows into the side holes of a catheter rather than out of the holes as shown in the experiments as shown in *Figure 3*. The diffusion loss in two scenarios may be different each other. This issue needs to be confirmed experimentally in the future. CFD studies on the minor hydraulic losses in biliary drainage catheters are also worthy of being attempted.

Recently, the flow rates in three commerical multipurpose pigtail drainage catheters at 30 mmHg presssure difference were measured in vitro with water by Macha, Thomas and Nelson in 2006.[19] The flow rates of water, three water solutions of guar gum across three pigtail

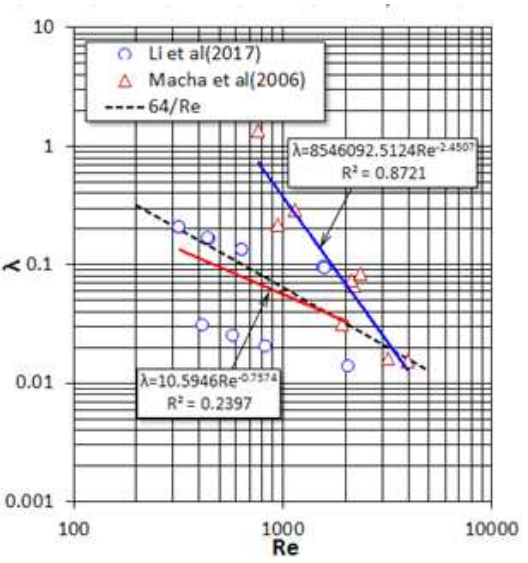

Figure 9. The experimental equivalent friction factors respectively by Macha, Thomas and Nelson[19] and Li, Ballard and D'Agostino[21] and fitted empirical correction of in terms of Reynolds number and its comparison with the analytical friction factor for a catheter.

cathetes (two multipurpose drainage catheters, one biliary drainage catherter) were in vitro measured at 12 cmH_2O pressure difference under side hole unobstructed and obstructed conditions, and it was identified that the number of side holes don't affect in vitro bilary catheter drainage.[21] The catheter geometrical parameters were presented in [19] and [21]. The flow rates in *Figure 4* in [19] and *Figure 2* in [21] for the unobstructed catheters were read and the equivalent frictiom factors were calculated by them with *Eq. (2)*, and the results are illustrated in *Figure 9*.

Clearly, the data points in two experiments are quite few and the Reynolds number is in the range of 300-4000, which is higher than that (20-1000) in *Figure 4*. The factors from the experimental data in[19] exhibit siginifcant variation. Even though the resgrssion equation for them is sightly below the analytical curve of $64/\mathrm{Re}$, its correlation coefficent is as small as 0.24.

The friction factors from the experimental data in [21] are considerably higher than the analytical curve as $\mathrm{Re} \leq 2000$. Nonetheless further experimental comfirmation is on demand.

Since there is one viscosity in the experiments and no information about the used bile rheology in [15], the bile in fluid mechanics model is considered Newtonian. Ooi et al measured the bile dynamic viscosity and found that the bile rheology of 20 out of 59 patients is Newtonian.[32] Reinhart, Naf and Werth found the bile of the majority samples from the common bile duct of 138 patients (64.5 %) are Newtonian.[33] These facts suggest that the Newtonian bile model seems to be reasonable. In some cases, however, the bile can be non-Newtonian,[32-35] therefore the correlation needs be updated in the future based on in vitro experimental data on non-Newtonian fluid flow through PTBD catheters.

The bile viscosity can vary significantly across patients, for example, the dynamic viscosity of gallbladder bile is 0.0177-0.08 Poise[32], and even higher in gallbladder bile of patients with cholesterol (0.05 Poise) and mixed stones (0.035 Poise) compared to hepatic bile (0.02 Poise) [31]. Therefore, more in vitro studies on bile flow through a catheter with a variety of viscosities need to be launched in the future.

Conculisons

Based on a set of existing in vitro bile flow measurements through the catheters made with five kinds of material and in various inner diameters and lengths for PTBD application under different pressure differences across the catheters, an equivalent friction factor was put forwarded and determined. Furthermore, an empirical correlation of bile flow rate through a catheter to pressure gradient, inner diameter and bile viscosity was developed and applied to clarify effects of variable catheter inner diameter and bile viscosity under the physiological bile pressure differences in obstructed common bile ducts. The effect of minor hydraulic losses in the catheters was identified. It was shown that the proposed equivalent friction factor was proportional to Reynolds number in a power of -0.654 rather than -1 for the fully developed limner flow in circular pipes. The bile flow rate through a catheter was proportional to inner diameter, kinematic viscosity, and pressure gradient in the powers of 3.2, -0.5 and 0.74, respectively. The minor hydraulic losses could be dominant as Reynolds number was higher than 100. Further work includes in vitro bile flow measurements at different viscosities, non-Newtonian bile effect on bile flow rate through a catheter and minor hydraulic losses estimation in biliary drainage catheters based CFD simulations.

Compliance with Ethical Standards

Funding: This study was not funded by any organizations.
Conflict of interest: The author has no conflict of interest.
Ethical approval: This article does not contain any studies with human participants or animals performed by the author.

REFERENCES

1. *Hoevels J, Lunderquist A, Ihse I.* Percutaneous transhepatic intubation of bile ducts for combined internal-external drainage in preoperative and palliative treatment of obstructive jaundice. Gastrointestinal Radiology, 1978,3: 23-31.
2. *Ring EJ, Husted JW, Oleaga JA, Freiman DB.* A multihole catheter for maintaining longterm percutaneous antegrade biliary drainage. Radiology, 1979,132:752-754.
3. *Nakayama T, Ikeda A, Okuda K.* Percutaneous transhepatic intubation of biliary tract. Gastroenterology, 1978,74(3):554-558.
4. *Ferrucci JT, Mueller PR, Harbin WP.* Percutaneous transhepatic biliary drainage. Diagnostic Radiology, 1980,135:1-13.
5. *Mueller PR, van Sonnenberg E, Ferrucci J.* Percutaneous biliary drainage: technical and catheter-related problems in 200 procedures. American Journal of Roentgenology, 1982,138:17-23.
6. *Mendez G, Russsell E, LePage JR, Guerra JR, Posniak RA, Trefler M.* Abandonment of endoprosthetic drainage technique in malignant biliary obstruction. American Journal of Roentgenology. 1984,143:617-622.
7. *Hamlin JA, Friedman M, Stein MG, Bray JF.* Percutaneous biliary drainage: complications of 118 consecutive catheterizations. Radiology, 1986,158:199-202.
8. *Joseph P, Bizer LS, Sprayregen SS, Gliedman ML.* Percutaneous transhepatic biliary drainage. JAMA, 1986,255:2763-2767.
9. *Sirinek KR, Levine BA.* Percutaneous transhepatic cholangiography and biliary drainage. Archives of Surgery, 1989,124:885-888.
10. *Weber A, Gaa J, Rosca B, Born P, Neu B, Schmid RM, Prinz C.* Complications of percutaneous transhepatic biliary drainage in patients with dilated and nondilated intrahepatic ducts. European Journal of Radiology, 2009,72:412-417.
11. *Knap D, Orlecka N, Judka R, et al.* Biliary duct obstruction treatment with aid of percutaneous transhepatic biliary drainage. Alexandria Journal of Medicine, 2016,52:185-191.
12. *Clark RA, Mitchell SE, Colley DP, Alexander E.* Percutaneous catheter biliary decompression. American Journal of Roentgenology, 1981,137:503-509.
13. *Yee CAN, Ho CS.* Complications of percutaneous biliary drainage: benign vs malignant diseases. American Journal of Roentgenology, 1987,148:1207-1209.
14. *Carrasco CH, Zornoza J, Bechtel WJ.* Malignant biliary obstruction: complications of percutaneous biliary drainage. Radiology, 1984,152:343-346.
15. *Kerlan RK, Stimac G, Pogany AC, Ring EJ.* Bile flow through drainage catheters: an in vitro study. American Journal of Roentgenology, 1984,143:1085-1087.
16. *Bret PM, Bretagnolle M, Fond A, Valette PJ, Bret P.* Use of large silicone catheters in patients in long-term percutaneous transhepatic biliary drainage. Cardiovascular and Interventional Radiology, 1986,9:57-58.
17. *Born P, Tripttrap A, Frimberger E, et al.* Long-term results of percutaneous transhepatic biliary for benign and malignant bile duct strictures. Scandinavian Journal of Gastroenterology, 1998, 33(5): 544-549.
18. *Park JK, Kraus FC, Haaga JR.* Fluid flow during percutaneous drainage procedures: An in vitro

study of the effects of fluid viscosity, catheter size and adjunctive urokinase. American Journal of Roentgenology, 1993,160:165-169.

19. *Macha DB, Thomas J, Nelson RC.* Pigtail catheters used for percutaneous fluid drainage: comparison of performance characteristics. Vascular and Interventional Radiology, 2006, 238(3):1057-1063.
20. *Ballard DH, Alexander JS, Weisman JA, Orchard MA, Williams JT, D'Agostino HB.* Number and location of drainage catheter side holes: in vitro evaluation. Clinical Radiology, 2015,70:974-980.
21. *Li AY, Ballard DH, D'Agostino HB.* Biliary drainage catheters fluid dynamics: In vitro flow rates and patterns. Diagnostic and Interventional Imaging, 2017,98:355-358.
22. *Ballard DH, Flanagah ST, Li H, D'Agostino HB.* In vitro evaluation of percutaneous drainage catheters: Flow related to connections and liquid characteristics. Diagnostic and Interventional Imaging, 2018,99: 99-104.
23. *Lee KH, Han JK, Kim KG, Byun Y, Yoon CJ, Kim SJ, Choi BI.* Clogging of drainage catheters: Quantitative and longitudinal assessment by monitoring intracatheter pressure in catheters and rabbits. Radiology, 2003,227(3): 833-838.
24. *Hamada T, Tsujino T, Isayama H, Hankuta R, Ito Y, Nakata R, Koike K.* Percutaneous transhepatic biliary drainage using a ligated catheter for recurrent catheter obstruction: antireflux technique. Gut and Liver, 2013,7(2):255-257.
25. *Nghiem DD.* Bile leakage after fracture of percutaneous transhepatic biliary drainage catheters. JAMA, 1984,251(7):892.
26. *Liu HT, Tseng HS, Lin YY, Liu CA.* Percutaneous transhepatic techniques for retrieving fractured and intrahepatically dislodged percutaneous transhepatic biliary drainage catheters. Diagnostic and Interventional Radiology, 2017,23:461-464.
27. *White FM,* Fluid Mechanics (7th edition), New York: McGraw-Hill Companies, Inc., 2011.
28. *Rodkiewicz CzM, Otto WJ, Scott G W.* Empirical relationships for the flow of bile. Journal of Biomechanics, 1979,12:411-413.
29. *White TT, Waisman H, Hopton D, Kavlie H.* Radiomanometry, flow rates, and cholangiography in the evaluation of common bile duct disease. American Journal of Surgery, 1972,123:73-79.
30. *van Sonnenberg E, Ferrucci JT, Neff CC, Mueller PR, Simeone JF, Wittenberg J.* Biliary Pressure: manometric and perfusion studies at percutaneous transhepatic cholangiography and percutaneous biliary drainage. Radiology, 1983,148:41-50.
31. *Jungst D, Niemeyer A, Muller I, Zundt B, Meyer G, Wilhelmi M, del Pozo R.* Mucin and phospholipids determine viscosity of gallbladder bile in patients with gallstones. World Journal Gastroenterology, 2001,7(2):203–207.
32. *Ooi RC, Luo XY, Chin SB, Johnson AG, Bird NC.* The flow of bile in the human cystic duct. Journal of Biomechanics, 2004,37(12):1913-1922.
33. *Reinhart WH, Naf G, Werth B.* Viscosity of human bile sampled from the common bile duct. Clinical Hemorheology and Microcirculation, 2010,44(3):177-182.
34. Coene PPLO, Gro*en AK, Davids PHP, Hardeman M, Tytgat GNJ, Huibregtse K.* Bile viscosity in patients with biliary drainage. Scandinavian Journal of Gastroenterology, 1994,29:757-763.
35. *Kuchumov AG, Gilev V, Popov V, Samartsev V, Gavrilov V. Non-Newtonian flow of pathological bile in the biliary system: experimental investigation and CFD simulations. Korea-Australia Rheology Journal, 2014,26(1):81-90.*

Wenguang Li
School of Energy and Power Engineering, Lanzhou University of Technology
Lanzhou, Gansu 730050, China
15810086985

ÍZÜLETEINK VÉDELMÉRE

SYNOCROM®
BIOENGINEERED HYALURONIC ACID

INTRAARTIKULÁRIS INJEKCIÓ

A SYNOCROM® intraartikuláris készítményekkel nagymértékben csökkenthető az ízületi fájdalom, és javítható az ízület mozgathatósága.

A SYNOCROM® termékek nagy tisztaságú, biofermentációs eljárással készült hyaluronsavat tartalmazó az ízületi folyadék pótlására alkalmazható injekciós kiszerelésű orvostechnikai eszközök. A termékek elsődlegesen a térdízületi arthrosis kezelésére szolgálnak, de egyéb ízületek degeneratív elváltozásai esetén is sikerrel alkalmazhatóak.

SYNOTABS®

PORCERŐSÍTŐ TÁPLÁLÉK KIEGÉSZÍTŐ

A SYNOTABS® filmtabletta kiszerelésben kapható táplálék kiegészítő, amely az egészséges ízületek és porcok fenntartásához járul hozzá. Speciális összetétele révén a SYNOTABS® filmtabletta tartalmaz minden olyan fontos összetevőt, ami segíti az ízületek védelmét.

PREMED PHARMA

PREMED PHARMA KFT.
CÍM 2040 Budaörs, Gyár u. 2.
TELEFON 06 23 889 700
FAX 06 23 889 710
E-MAIL info@premedpharma.hu
WEB www.premedpharma.hu

Gerincalak és izomaktivitás együttes változása törzserő-tesztek során fiatal kosárlabdázók körében

Petró Bálint[1], Gál-Pottyondy Anna[2], Kiss Rita M.[1]

[1] Budapesti Műszaki és Gazdaságtudományi Egyetem, Mechatronika, Optika és Gépészeti Informatika Tanszék

[2] Testnevelési Egyetem

rita.kiss@mogi.bme.hu

DOI: 10.17489/biohun/2019/1/02

Absztrakt

A mindennapi és a sportéletben egyaránt fontos a törzsizmok és más testtartásért felelős izmok megerősítése és egyensúlyának biztosítása. A testtartás izmainak tesztelésére jól alkalmazható a plank-teszt, mely a fekvőtámaszhoz hasonló, csak hajlított alkartámaszban kezdődik és ennek a helyzetnek az egy percig történő megtartása. Előnye, hogy könnyen elvégezhető és nem igényel eszközt, ugyanakkor a teszt kiértékelése leggyakrabban csak szubjektíven, szemrevételezéssel történik. Ezért kialakítottunk egy új mérési protokollt a gerinc alakjának és az izomaktivitás változásának egyidőben való követésére.

A protokoll tesztelésére 11 fiú kosárlabdázó (13-17 év) részvételével végeztünk méréseket; a feladat egy percig tartó plank-teszt volt. A gerinc alakját tövisnyúlványokra helyezett jelölők optikai követésével állapítottuk meg, melyből a gerincgörbületi szögek (kyphosis és lordosis) számíthatók minden időpontra. Felületi elektromiográfiával mértük 11 izom aktivitását; a medián frekvencia csökkenésének számításával megállapítottuk az izomfáradás mértékét.

A gerincszögek változása a gyakorlat első és utolsó 10 másodperce között minden esetben a kyphosis (jellemzően nagymértékű) növekedését mutatta; a lordosis vagy kismértékben csökkent, vagy nagymértékben nőtt. Ez azt mutatja, hogy a plank-teszt során az egyes résztvevők különböző módokon fáradnak el, melyek indikálhatják különböző stabilizáló izmok gyengeségét.

Az EMG medián frekvenciája a gyakorlat során jellemzően vagy közel állandó, vagy egyenletesen csökkenő volt a vizsgált izmokban (szignifikánsan fáradt a m. gluteus maximus, az erector spinae iliocostalis, a rectus abdominis longus és az obliquus externus abdominis), ám néhány izom mutatott hullámzó aktivitást is. Szignifikáns korrelációt a m. rectus femoris fáradása és a gerincgörbületek növekedése között találtunk. További kutatási lehetőséget ad a protokoll elvégzése homogén életkorú, különböző sportot űző csoportok részvételével.

Kulcsszavak: elektromiográfia, izomfáradás, gerincgörbületek, törzserő, core izmok

Concurrent changes in spinal curvatures and muscle activities during postural muscle testing among young basketball players

Abstract

Strengthening postural and core muscles and ensuring their balance is vital in everyday and sports life as well. For functional testing of postural muscles, the plank-test can be used which consists of holding the plank (prone bridge) position for an amount of time, e.g. 1 minute. This test is easy to administer and

requires no equipment; however, evaluation is usually done only visually, in a subjective manner. This motivated the development of a novel measurement protocol simultaneously recording spinal curvatures and muscle activations.

Testing of the protocol was done involving 11 young boy basketball players (aged 13-17 years); the task was holding the plank position for one minute. Spinal curvatures were recorded by placing optical motion capture markers on eleven spinous processes from which the curvature angles (kyphosis and lordosis) could be obtained for each video frame. Surface electromyography was used to measure activities of 11 muscles; muscle fatigue was obtained by calculating the decrease in median frequency of the electric signal.

The changes in curvature comparing the first and last 10 seconds of the tests showed for every participant a (usually large) increase in kyphosis values; lordosis values either decreased to a small extent or increased to a large extent. This shows that during the plank-test, the fatiguing process is can differ among individuals which may indicate the lack in power of different postural muscles.

The median frequencies of EMG signals generally either stayed constant during the test or showed a steady decrease. Significant fatigue was detected for the m. gluteus maximus, the erector spinae iliocostalis, the rectus abdominis longus and the obliquus externus abdominis. Some muscles showed a fluctuation in activity. Comparing muscle fatigue and curvature changes, only the m. rectus femoris showed a significant correlation. Further research should be carried out involving a more homogeneous participant group and participants from other sports as well.

Keywords: electromyography, muscle fatigue, spinal curvatures, core strength, core muscles.

Bevezetés

A törzsizmoknak és a testtartásért felelős egyéb izmoknak szinte minden mozgás közben aktív, stabilizáló szerepük is van. Ezen izmok megfelelő erőállóképessége és izomegyensúlya egyaránt fontos. Elengedhetetlen a törzsizmok megerősítése a helyes testtartás és a magas terhelhetőség érdekében. Erős törzsizomzattal gyorsabban, pontosabban tudják a mozgásokat végrehajtani a sportolók. Magasabb szintű sporteredmény eléréséhez elengedhetetlen a súlyzós edzések edzésprogramba való beépítése. Ennek azonban szigorú előfeltételei és szabályai vannak, mint a csontosodási folyamatok befejeződése, a közel végleges testarányok kialakulása, a gyakorlatok saját testsúllyal történő tökéletes kivitelezése.

A csont- és izomrendszer egészséges fejlődését megtartó, elősegítő edzések tervezéséhez szükséges a sportolók aktuális fiziológiás állapotának ismerete. A törzsizmok csökkent állóképessége és az alsó végtag fáradásos sérülései szignifikánsan összefüggnek.[1] Ugyanakkor Nesser és munkatársai szignifikáns, de nem erős összefüggést találtak a törzserő és az általános erőt mérő változók között sprintfutás, ingafutás, guggolás és fekvenyomás gyakorlatokat vizsgálva.[2] Kiemelik, hogy a törzs izmai egy egységet alkotnak, így egységben, több izomcsoportot együttesen vizsgálva célszerű összehasonlítani azok működését sportspecifikus tesztekkel. A gerinc és az azt körülvevő izmok állapotának felmérése a sérülések rizikójának becslésénél és az általános terhelhetőség megállapításánál is fontos szerepet játszik.[2]

A törzsizmok erejének tesztelésére elterjedten használnak statikus, izometrikus terhelést jelentő teszteket, gyakorlatokat.[3–6] Ezen egyszerű tesztek sportéletben használatának gyakor-

lati előnye, hogy könnyen megismételhetők és alacsony eszközigényűek. Sok esetben azonban csak a feladatot végeztető gyógytornász vagy más szakember megtekintése alapján értékelik a tesztet, tehát egyelőre hiányoznak a feladatok objektív, műszeres kiértékelési lehetőségei. Népszerűségük miatt azonban tudományos kutatások is vizsgálták már ezeket a gyakorlatokat. A törzserőtesztek kiértékelésében a mozgás kinematikai mérése mellett az izomaktivitás felületi elektromiográfiás (EMG) vizsgálatát alkalmazzák. Sportolók törzsizomzatának aktuális állapotának megfelelő és hiteles felmérésére alkalmas például a módosított Matthias-teszt[3] vagy a plank-teszt is.[4–6] A plank-pozíció egyperces megtartása a core izomcsoportok állóképességi munkáját igénylő saját testsúllyal történő feladat. Ugyanakkor Tillaar és munkatársa a rectus abdominis és az external obliqe izmok esetében hasonló aktivitást figyelt meg a hat ismétléses maximális guggolás és az egyperces plank gyakorlatok kivitelezése közben.[7]

Az utánpótlás korú sportolóknak nemcsak a növekvő edzés- és versenyterheléssel kell megküzdeniük, hanem testük gyors ütemű változásával, növekedésével is. Serdülőkorban nagy figyelmet kell szentelni a kondicionális képességek megfelelő fejlesztésére. A hosszútávú és magas szintű sporteredmény eléréséhez elengedhetetlen, hogy a sportágspecifikus erősítések mellett helyet kapjanak a helyes testtartást és izomegyensúlyt elősegítő feladatok is. Jellemzően az aszimmetrikus terheléssel járó sportágak sportolói a veszélyeztettek, azonban a nem tipikus testalkatot igénylő sportokat is, mint például a kosárlabdát, kiemelten kell kezelni. Lark és munkatársai megmutatták, hogy a plank-teszt alkalmas aktív kosárlabdázók törzsizomzatának felmérésére.[8] Ezért célul tűztük ki egy vizsgálati protokoll kifejlesztését és tesztelését, amely lehetővé teszi a plank-teszt objektív kiértékelését. A testtartás objektív méréséhez a gerinc alakját, és annak változását mérjük; emellett vizsgálni szeretnénk a pozíció megtartásában leginkább szerepet játszó izmok fáradását is. Hasonló elrendezésű méréseket nemrégiben kezdtek kutatásokban használni.[9] A gerinc alakjának folytonos követése lehetséges fényvisszaverő jelölők (markerek) bőrre való felhelyezésével.[10] A csigolyatövisnyúlványokra helyezett jelölők pozícióját optikai mozgáskövető (motion capture, MoCap) rendszerrel meghatározhatjuk minden képkockán; az ezekre illesztett görbe közelíti a gerincoszlop alakját. Ezzel a módszerrel abszolút gerincgörbületi értékek csak bizonytalansággal állapíthatók meg, azonban alkalmas a görbületi szögértékekben történő változások meghatározására.[10,11] A módszert korábban megvalósítottuk a BME MOGI Tanszék Mozgásvizsgáló Laboratóriumában.[12] A gerincgörbületek mérésével párhuzamosan érdekesek lehetnek az egyes izmok fáradásai is. A fáradás mértékének megállapításához az EMG-jelek megfelelő szűrése[13] után az elektromos jel medián frekvenciáját számíthatjuk, amelynek csökkenése indikálja az izomfáradást.[14,15]

Jelen kutatás célja egy olyan vizsgálati módszer kidolgozása, amellyel egyidejűleg meghatározható a gerinc alakjának változása és az ehhez kapcsolódó izmok aktivitása, fáradása. A módszer kiterjeszthető egyéb ízületek szögének változására, így bármilyen mozgás vizsgálatára is. Mostani, előzetes méréseinket fiatal kosárlabdázók körében végeztük el.

Módszerek

Résztvevők

Méréseinken a Szolnoki Kosárlabda Akadémia 11 fiú sportolója vett részt. A résztvevők életkora 13-17 év (átlag 14,6 év), testmagassága 153-199 cm (átlag 181 cm), testtömege 37-81 kg (átlag 63,1 kg). Méréseinket a BME MOGI Tanszékének Mozgásvizsgáló laboratóriumá-

ban végeztük, három alkalomra elosztva. A mérés előtt kikérdeztük a résztvevőket múltbéli és jelenlegi sportolási szokásaikról, aktuális sportterhelésükről, a csapatban betöltött pozíciójukról, valamint aktuális állapotukról: sportoltak-e előző nap, milyen állapotban érzik magukat. Néhány résztvevő enyhe izomlázról számolt be előző napi sportolás miatt.

Mérési protokoll

Az érzékelők és jelölők megfelelő felhelyezése és tesztelése után a résztvevő a MoCap rendszer mérőterében, a padlón elhelyezett polifoam szőnyegen elhelyezkedik. Felveszi a fekvőtámaszhoz hasonló plank-pozíciót *(1. ábra)*, behajlított karokkal, alkarjára támaszkodva; az alkarok párhuzamosak a gerinccel. A test egyenes; a tarkó, a vállak közti háti szakasz, a keresztcsont, a térdek és a bokák egy vonalon helyezkednek el. Az instrukció: A szabályos plank-pozíciót tartsa meg egy percig. A szabályos pozíció felvételével indult a 60 s-os mérés. A feladat megkezdése után már nem kapott további instrukciót a játékos, még abban az esetben se, ha már nem volt szabályos a feladat kivitelezése.

1. ábra. Plank-pozíció, mérési elrendezés

Gerinc alakjának mérése

A gerinc alakjának és a test pozíciójának méréséhez retroreflektív markereket helyeztünk el a résztvevőn. A markerek térbeli pozícióját egy 18 kamerás OptiTrack© Motive (NaturalPoint Inc., Oregon, USA) mozgásvizsgáló (MoCap) rendszerrel követtük nyomon, 100 Hz-es mintavételezéssel. Összesen 10 csigolya processus spinosusait jelöltük meg[12] *(lásd 1. ábrán)*, ezek: C6, T1, T4, T6, T8, T10, T12, L2, L4 és L5. További markereket helyeztünk el a sacrumon, a jobb- és baloldali fültövön, vállcsúcson, könyök és csukló laterális bütykén, a nagytomporokon, a térd és boka laterális oldalain, amelyek a jobb követhetőség biztosították, adataikat nem használtuk fel.

Az adatfeldolgozás során a mért markerpozíciókat aluláteresztő szűrővel, 6 Hz-es vágási frekvenciával simítottuk. A gerincalak meghatározásához a 10 tövisnyúlványon lévő markerre térbeli spline görbét illesztettünk a négyzetes hibaérték minimalizálásával. A lumbális lordózis (LL) és a thorakális kyphosis (TK) szögek definíciószerűen a mért pontokra illesztett görbe T1, T12, L5 processus spinosusokat reprezentáló pontoknál behúzott érintők által bezárt szögek.

Izomaktivitás mérése felületi elektromiográfiával – vizsgált izmok, mérési protokoll, jelfeldolgozás

Az izomaktivitás Telemyo típusú felületi, bipoláris EMG adatgyűjtő berendezéssel (Noraxon Inc., Scottsdale, AZ, USA) történt. Az adatgyűjtő 16 vezetékes csatornát használ, valamint elérhető hozzá egy rádiófrekvenciás adóvevő is. Az adóvevő párja egy mobilis felvevő egység, amelyhez 16 csatorna csatlakoztatható. A felvevőben tízszeres erősítés található, a jel/zaj viszony 65 dB-nél nagyobb. A felvevő összegzett szűrési sávja 0-1150 Hz; a mintavételezési frekvencia 2 kHz. Az adatgyűjtő a hozzá tartozó gyári szoftver segítségével kapcsolódik a mérést vezérlő számítógéphez.

A bipoláris, felületi elektródákat a SENIAM[16] ajánlásait követve helyeztük el. A gerincen eredő izmok közül két felületes izmot vizsgáltunk, ezek a m. erector spinae longissimus és

a m. erector spinae iliocostalis, melyek a gerinc legfőbb feszítő izmai. A hasizmok közül szintén kettőt vizsgáltunk, ezek a m. obliquus externus abdominis és a m.rectus abdominis, melyek fő feladata a hasűri nyomás fenntartása és az alsó és felső testfél izomláncai közötti kapcsolat kialakítása. A medencefenék izmai közül a m. gluteus maximus és m. gluteus medius izmokat mértük. Előbbi, a maximus a csípőízület feszítője, ezáltal az egyenes testtartás legfőbb biztosítéka, míg a medius a comb abductora és belső rotátora, így fekvőtámaszban is rögzítő szerepe van. A térdízület mozgatását végző izmok közül a m. rectus femoris-t (csípőízületi flexio), a m. adductor longus-t (comb adductora) és a m. biceps femoris-t (térdízület flexio) mértük. A bokaízület mozgatásában részt vevő izmok közül a m. tibialis anterior-t (a lábfejet bokából lábháti irányba hajlítja) és a m. gastrocnemius medialis-t (térd flexio, boka plantarflexio) mértük. Erről a mérési elrendezésről korábban beszámoltunk.[17] A földpontot a térdkalácson helyeztük el.

A használt elektródák Ambu gyártmányú (Ballerup, Dánia) „BlueSensor N" típusú, egyszer használatos csecsemőkre méretezett EKG-elektródák voltak, melyek ezüst/ezüstklorid anyagúak. Két egymás mellé helyezett elektróda közt 2 cm távolság volt. Az elektródák felhelyezése előtt a területet frissen leborotváltuk, a legfinomabb dörzspapírral a bőr felületét lecsiszoltuk, majd egy alkoholos bőrfertőtlenítő folyadék és vatta segítségével a bőrön található maradék szennyeződést is eltávolítottuk. Az elektródákat és azokat a felvevővel összekötő kábeleket leukoplaszttal rögzítettük a bőrhöz. A kontaktus ellenőrzésére az egyes izmok megfeszítésére, terhelésére kértük a résztvevőt a SENIAM modellben megadott testhelyzetekben.

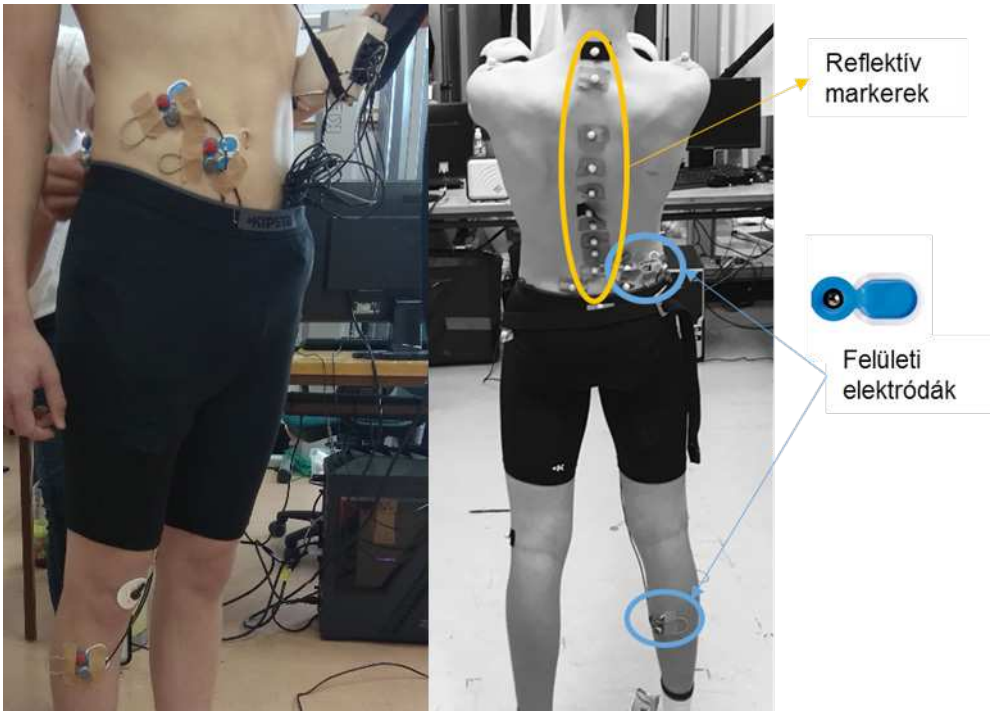

2. ábra. Felhelyezett felületi elektródák és reflektív markerek

Az EMG-jelek, mint minden fiziológiás elektromos jel mérése során zajokkal terheltek. Az alacsony frekvenciás zajok (0-20 Hz) az elektróda, a bőr vagy az elektródához csatlakozó kábelek elmozdulásából ered. Ezek a frekvenciakomponensek különösen instabilak, mivel ezeket a motoregységek tüzelési sebességének kvázi-véletlenszerű jellege befolyásolja. A jel összetevőinek instabil jellegéből adódóan tanácsos ezeket zajnak tekinteni és eltávolítani őket a jelből. A helyiségben lévő hálózati 50 Hz-es frekvencia szintén könnyen megjelenik a mért jelben. Az is ismert, hogy 500 Hz fölött már nem számíthatunk izomaktivitás eredetű EMG-jelre, hiszen ennél sűrűbben tipikusan nem fordulnak elő akciós potenciálok. A törzs izmaira tett elektródák sok esetben érzékelik a szívből jövő EKG jeleket, ami az izmok tekintetében szintén zajnak tekinthető, így azok kiszűrése is indokolt. Ennek megfelelően a mért elektromos jeleken szűréseket végeztünk: az EKG-jel kiszűrését, felüláteresztő szűrést 20 Hz-es vágási frekvenciával; sávzáró szűrést 45-55 Hz között, illetve aluláteresztő szűrést 500 Hz-es vágási frekvenciával.

A frekvenciatartományi szűrések elvégzése után a mért jel további, tüskeszerű műhibákkal volt terhelt. Ezek ritkán, csak egymástól több másodpercnyi távolságra helyezkedtek el, és mindössze 4-8 minta hosszúak voltak, azonban amplitúdóban a jel többi részének sokszorosát jelentették és a medián frekvencia számítását irreálisan befolyásolták. Ezeket a tüskéket hibás mért értéknek tekintve, nullával helyettesítettük.

A MoCap rendszerrel való mérés időbeli szinkronizálásához, a mérés kezdetének illesztéséhez a MoCap rendszer megfelelő kezelőszervén lévő szinkronizáló kimenetet vezetékkel összekötöttük az EMG adatgyűjtő egyik csatornájával. A vezetéken alapértelmezésben alacsony feszültségszintű jel van, mely a MoCap rendszer felvételének indításakor magas szintre ugrik, így ez az él egyértelműen jelöli az indítást.

Vizsgált paraméterek

Az izomfáradás számszerű jellemzésére az EMG-vel mérhető izomaktivitás medián frekvenciájának megváltozását használtuk.[15] Az egyenként 60 másodperces felvételeket 3 s hosszú, egymással 50 %-ban átfedő szakaszokra bontva számítottuk a medián frekvenciát, a szakaszok középpontjához rendelve. A 60 s hosszú felvételekre kapott medián frekvencia értékekre lineáris regressziót illesztettünk. Így a regressziós egyenes meredeksége mutatja a medián frekvencia átlagos csökkenését, esetlegesen növekedését. Ezt a csökkenő meredeksé-

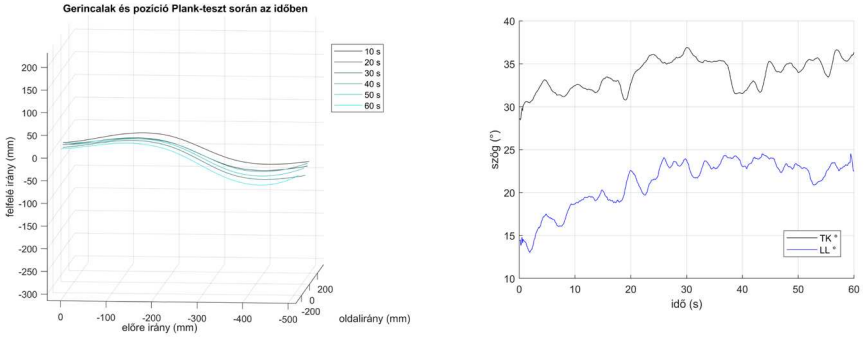

3. ábra. Gerincalak változása plank-teszt során egy résztvevőre

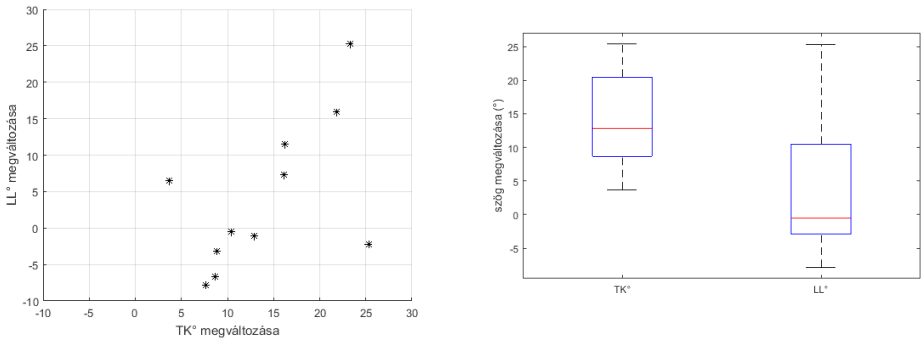

4. ábra. Szórásdiagram és dobozábra a TK és LL szögek megváltozásáról a plank-teszt eleje és vége között a csoportban

get tekintjük izomfáradásnak. Az egyes izmok összehasonlíthatósága érdekében a medián frekvenciákat azok maximumával normáltuk 0 és 100% közé, így az egyenes meredekségének számértéke is így értelmezendő. Negatívabb meredekség nagyobb mértékű izomfáradásnak felel meg.

A gerincalakot leíró két szög, a TK és LL értékeléséhez a 60 s hosszú plank gyakorlat alatt az első és utolsó 10 s-es szakaszon mért szögek átlagát és szórását hasonlítottuk össze, minden résztvevőt saját magával. A különbség statisztikai szignifikanciáját Wilcoxon-féle előjeles rang-teszt alkalmazásával vizsgáltuk. Szintén összehasonlítottuk a TK és LL szög gyakorlat során történt megváltozását az egyes izmok fáradásával, itt Spearman-féle korrelációs együtthatót számítottunk.

Eredmények

A MoCap rendszer használatával a gerincalak a gyakorlat végzése során végig meghatározható *(példa a 3. ábrán)*, amelyet videóként megtekintve értékelhető a gerincben bekövet-

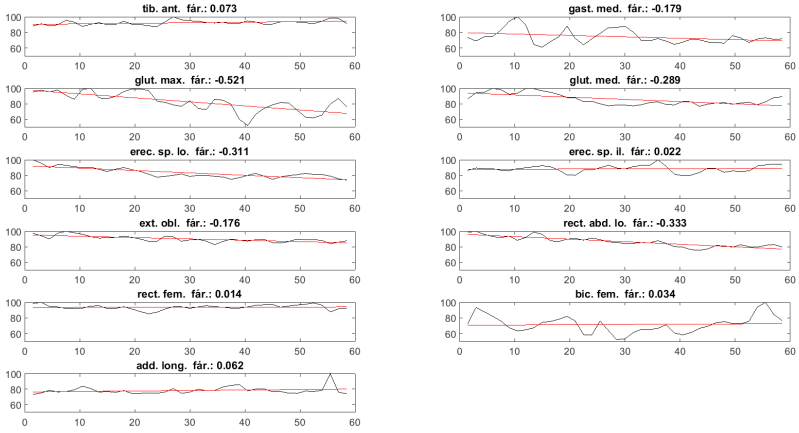

5. ábra. A vizsgált izmok mediánfrekvenciája plank-teszt során egy résztvevőre

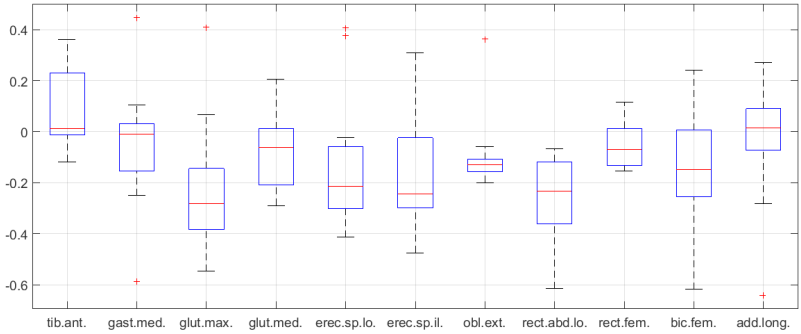

6. ábra. A vizsgált izmok fáradása a csoportban

kező változás. Ez a gerincszögeket ábrázolva szintén követhető *(példa a 3. ábrán)*. A gerincszögek változása a gyakorlat első és utolsó 10 s-a között minden esetben a TK (jellemzően nagymértékű) növekedését mutatta; az LL szög vagy kismértékben csökkent, vagy nagymértékben nőtt *(4. ábra)*. A TK megváltozása erősen szignifikáns ($p<0{,}001$), míg az LL megváltozása a kétféle viselkedés miatt nem szignifikáns ($p=0{,}4659$) a csoportban. A TK és LL megváltozása nagymértékben korrelált: $rho=0{,}57$ ($p=0{,}07$), két erősen kiugró adatpont mellett *(4. ábra)*.

Az EMG medián frekvenciája a gyakorlat során jellemzően vagy közel állandó, vagy egyenletesen csökkenő volt a vizsgált izmokban, ám néhány izom mutatott hullámzó aktivitást is *(példa az 5. ábrán)*. A csoport tagjai közül leggyakrabban ilyen hullámzó aktivitást mutatott rendre a m. gluteus maximus, a m. gluteus medius, a m. gastrocnemius medialis és a m. biceps femoris.

Az egész csoportra vetítve az egyes izmok jellemző fáradását mutatja a *6. ábra*; a statisztikai szignifikanciaértékeket az *1. táblázatban* foglaltuk össze. Egyöntetűen fáradást mutatott a m. gluteus maximus ($p=0.032$), az erector spinae iliocostalis ($p=0.102$) és a rectus abdominis longus ($p=0.001$), valamint kismértékben a m. obliquus externus abdominis ($p=0.054$) is.

A gerincszögek megváltozása és az izmok fáradása között kevés szignifikáns korreláció volt felfedezhető *(2. táblázat)*. Szignifikáns korrelációt csak a m. rectus femoris és a m. gastrocnemius medialis mutatott. A m. rectus femoris esetében a korreláció negatív, azaz a nagyobb fáradás (csökkenő aktivitás) nagyobb szögváltozást eredményezett a gerincben. Ezzel szemben a m. gastrocnemius medialis pozitívan korrelált, azaz nagyobb aktivitás esetén a szögváltozás nagyobb volt. Feltételezhetően ez a célzott testtartástól való eltérés miatt egy kompenzációs folyamatot jelez.

izom	**tib ant**	**gast med**	**glut max**	**glut med**	**erec sp lo**	**erec sp il**
p-érték	0.240	0.465	0.032	0.123	0.240	0.102
izom	**obl ext**	**rect abd lo**	**rect fem**	**bic fem**	**add lon**	
p-érték	0.054	0.001	0.206	0.123	1.000	

1. táblázat. A vizsgált izmok fáradásának szignifikanciája a csoportban

izom	tib ant	gast med	glut max	glut med	erec sp lo	erec sp il
TK	0.53*	0.77***	-0.02	0.21	0.46	0.45
LL	-0.06	0.55*	-0.16	0.15	0.17	0.45
izom	obl ext	rect abd lo	rect fem	bic fem	add lon	
TK	0.44	-0.35	-0.61**	0.35	-0.15	
LL	0.14	0.11	-0.68**	0.27	0.07	

2. táblázat. Korrelációs együttható a gerincszögek megváltozása és az izmok fáradása között
*p<0.1, **p<0.05, ***p<0.01

Megbeszélés

Jelen munka célja a a gerincgörbület változásának és a testtartásért felelős izmok fáradásának mérése volt egyperces plank-teszt során. A mozgáselemző rendszer felvételei alapján a processus spinosusok által leírt görbék változásait a két gerincgörbület (kyphosis és lordosis) formájában numerikusan rögzítettük, és a teszt eleje és vége közti pozíciókban lévő különbséget vizsgáltuk. Míg a TK minden esetben megnövekedett, az LL bizonyos résztvevőknél csökkent vagy stagnált, míg másoknál nagymértékben megnőtt. Felületi EMG-vel detektált jelek alapján az izmok aktivációs szintjének változását, illetve a kontrakciók során bekövetkező fáradást is kimutattuk. Szignifikáns fáradást mutatott a csoportot tekintve a m. gluteus maximus, az erector spinae iliocostalis, a rectus abdominis longus és az obliquus externus abdominis. Szignifikáns korrelációt a gerincgörbületek növekedése és az izomfáradás között csak a m. rectus femoris esetében találtunk.

Az egyperces plank-teszt során minden esetben észlelhető volt jelentősebb testtartásbeli változás *(4. ábra)*, tipikusan a TK nagymértékű növekedése. A gyakorlat során az LL esetében egyénenként változóan előfordult a lágyéki hátszakasz kiegyenesedése, valamint a medence beejtésével a nagyfokú görbületi növekedés is *(4. ábra)*. Ez azt mutatja, hogy a plank-teszt során az egyes résztvevők különböző módokon fáradnak el, melyek indikálhatják különböző stabilizáló izmok gyengeségét. Bohannon és munkatársai szintén kifáradásig végzett plank-teszt során a fáradás többféle megjelenését figyelték meg.[18] A vizsgálati személyek (n=103) saját elmondás alapján 11 féle módon indokolták a gyakorlat abbahagyását. Első helyen szerepelt a remegés, második helyen a hátfájás, de megjelent többek között a has és a comb fáradása is. Ezért plank-teszt során a gerincgörbület műszeres regisztrálása segítség lehet a törzsizmok állapotfelmérésében. Czaprowski és munkatársai plank-teszt során a m. rectus abdominis, m. obliquus externus, m. internal oblique/m. transversus abdominis izmok EMG aktivitását vizsgálták.[19] Vizsgálataik során az m. obliquus externus izomnál figyelték meg a legnagyobb (42.3±19.5 %MVC) aktivitást. A m. rectus abdominis és a m. internal oblique/m. transversus abdominis esetében jóval alacsonyabb izomaktivitást mértek (18.1±9.1 és 18.5±12.2 %MVC). Ez az eredmény a mi eredményeinktől különbözik, mivel a m. rectus abdominis-nél egyértelmű fáradást figyeltünk meg míg az m. obliquus externus izomnál csak kismértékben jelent meg a mediánfrekvencia csökkenése. Escamilla és munkatársai az m. rectus abdominis alsó részén (40±10 %MVC) és a m. obliquus externus esetében (40±20 %MVC) viszont közel azonos izom aktivitást figyeltek meg.[20] Ezek alapján arra következtethetünk, hogy a fent említett izmok mindenképpen jelentős szerepet játszanak a plank testhelyzet megtartásában. Pontos szerepük és jelentőségük felmérése a gyakorlatban még további vizsgálatot igényel.

Az eredmények alapján a statikus gyakorlat alatt a gerinc helyzetének és görbületeinek, valamint az izmok aktiváció szintjének időbeli változása, azaz a fáradás, mind kinematikailag, mind izom aktivációs oldalról kimutatható. A gerincszögek és az izmok medián frekvenciájának összevetése alapján például a *3. ábrán* látható 40 s környéki TK billenés a m. gluteus maximus és a m. erector spinae iliocostalis hirtelen aktivitáscsökkenésével indokolható *(5. ábra)*.

A teljes gyakorlat alatti izomfáradást a gerincgörbület változásával összevetve megállapítható, hogy érdekes módon csak a m. rectus femoris mutatott szignifikáns, nagymértékű korrelációt. Feltételezhető, hogy egy ilyen hosszúságú gyakorlat során többször cserélődnek a jobban aktivált és éppen pihenő izmok, így is csökkentve a fáradást. Lehetséges, hogy az izmokat funkció szerint csoportosítva, ezen csoportok összegzett aktivitása már mutatna korrelációt a testtartás változásával.

Mivel a vizsgálat célja a mérési eljárás ellenőrzése volt, amelyet széles célcsoporttal kívántunk megtenni, a vizsgálat elsődleges korlátja az alacsony létszámú, erősen inhomogén résztvevői csoport. További korlátot nyújtott, hogy csak felületi elektródákat használhattunk, így a mélyebb tartóizmok fáradását nem regisztrálhattuk.

A kutatás következő lépésében a létszámot növelve, homogén életkorú csoportokban folytatnánk a vizsgálatot. A vizsgálódás kiterjeszthető más törzserőt mérő tesztekre is, mint például a Matthias-teszt. Fontos feladat az EMG regisztrátumon megjelenő, nem a motoros egységekből jövő jelek zajszűrési eljárásának tökéletesítése. További lehetőség a gerincalak folytonos megváltozása és az izomfáradás közötti kapcsolat meghatározásához keresztkorreláció számítása a gerincszögek és az mediánfrekvencia adatok között. Az analízis kiterjeszthető oly módon, hogy az izmokat funkcionális csoportonként vizsgáljuk, így kimutathatóvá válhat az akaratlagos és akarat nélküli terhelésmegosztás az egyes tartóizmok között. Kiemelendő, hogy a módszer tovább fejleszthető tetszőleges ízületi szögek megváltozásának követésére is.

Összefoglalva megállapíthatjuk, hogy az izomfáradás elemzése kimutatta azon főbb testtartásért felelős izmok fáradását, amelyeket a plank-teszt megcéloz, míg a gerincgörbületi eredmények arra utalnak, hogy a lumbális gerincszakasz tartásának megváltozása lehet a teszt sikeres vagy sikertelen elvégzésének mutatója.

IRODALOMJEGYZÉK

1. *De Blaiser C, De Ridder R, Willems T, Vanden Bossche L, Danneels L, Roosen P.* Impaired Core Stability as a Risk Factor for the Development of Lower Extremity Overuse Injuries: A Prospective Cohort Study. Am J Sports Med. 2019;1–9.
2. *Nesser TW, Huxel KC, Tincher JL, Okada T.* The relationship between core stability and performance in division i football players. J Strength Cond Res. 2008;22(6):1750–4.
3. *Betsch M, Wild M, Jungbluth P, Thelen S, Hakimi M, Windolf J, et al.* The rasterstereographic-dynamic analysis of posture in adolescents using a modified Matthiass test. Eur Spine J. 2010;19(10):1735–9.
4. *Ekstrom RA, Donatelli RA, Carp KC.* Electromyographic Analysis of Core Trunk, Hip, and Thigh Muscles During 9 Rehabilitation Exercises. J Orthop Sport Phys Ther. 2007;37(12):754–62.
5. *Tong TK, Wu S, Nie J.* Sport-specific endurance plank test for evaluation of global core muscle function. Phys Ther Sport. 2014;15(1):58–63.
6. *De Blaiser C, De Ridder R, Willems T, Danneels L, Vanden Bossche L, Palmans T, et al.* Evaluating abdominal core muscle fatigue: As-

sessment of the validity and reliability of the prone bridging test. Scand J Med Sci Sport. 2018;28(2):391–9.

7. *Van den Tillaar R, Saeterbakken AH.* Comparison of Core Muscle Activation Between a Prone Bridge and 6-RM Back Squats. J Hum Kinet. 2018;62(1):43–53.
8. *Lark SD, Dickie JA, Faulkner JA, Barnes MJ.* Muscle activation and local muscular fatigue during a 12-minute rotational bridge. Sport Biomech [Internet]. 2018;3141:1–12. Available from: http://doi.org/10.1080/14763141.2018.1433870
9. *Schellenberg F, Schmid N, Häberle R, Hörterer N, Taylor WR, Lorenzetti S.* Loading conditions in the spine, hip and knee during different executions of back extension exercises. BMC Sports Sci Med Rehabil. 2017;9(1):5–8.
10. *Zemp R, List R, Gulay T, Elsig JP, Naxera J, Taylor WR, et al.* Soft tissue artefacts of the human back: Comparison of the sagittal curvature of the spine measured using skin markers and an open upright MRI. PLoS One. 2014;9(4):1–8.
11. *Schmid S, Studer D, Hasler CC, Romkes J, Taylor WR, Brunner R, et al.* Using skin markers for spinal curvature quantification in main thoracic adolescent idiopathic scoliosis: An explorative radiographic study. PLoS One. 2015;10(8):1–12.
12. *Takács M, Gál-Pottyondy A, Petró B, Rudner E, Váradi A, Kiss RM.* Ultrahangalapú gerincvizsgáló eszközzel és optikaialapú mozgáskövető rendszerrel végzett gerincvizsgálatok eredményeinek összevetése. In: A Magyar Gerincgyógyászati Társaság 2019 évi Tudományos Ülése. 2019. p. 17–8.
13. *Horváth M, Fazekas G.* Metodikai összefoglaló mozgáskárosodás felmérése elektromiográfiával – a kineziológiai emg. Ideggyogy Sz. 2003;56(11–12):360–9.
14. *Yoshitake Y, Ue H, Miyazaki M, Moritani T.* Assessment of lower-back muscle fatigue using electromyography, mechanomyography, and near-infrared spectroscopy. Eur J Appl Physiol. 2001;84(3):174–9.
15. *Cifrek M, Medved V, Tonković S, Ostojić S.* Surface EMG based muscle fatigue evaluation in biomechanics. Clin Biomech. 2009;24(4):327–40.
16. *Hermens HJ, Freriks B, Disselhorst-Klug C, Rau G.* Development of recommendations for SEMG sensors and sensor placement procedures. J Electromyogr Kinesiol [Internet]. 2000 [cited 2018 Aug 13];10(5):361–74. Available from: www.elsevier.com/locate/jelekin
17. *Gál-Pottyondy A, Takács M, Petró B, Kisrákói A, Kiss D, Kiss RM.* Egyperces statikus gyakorlatok alatt , optikai mozgáskövető rendszerrel végzett gerincvizsgálatok kineziológiai elektromiográfiával egybekötve. In 2019. p. 5–6.
18. *Bohannon RW, Steffl M, Glenney SS, Green M, Cashwell L, Prajerova K, et al.* The prone bridge test: Performance, validity, and reliability among older and younger adults. J Bodyw Mov Ther. 2018;22(2):385–9.
19. *Czaprowski D, Afeltowicz A, Gebicka A, Pawłowska P, Kedra A, Barrios C, et al.* Abdominal muscle EMG-activity during bridge exercises on stable and unstable surfaces. Phys Ther Sport. 2014;15(3):162–8.
20. *Escamilla RF, Lewis C, Pecson A, Imamura R, Andrews JR.* Muscle Activation Among Supine, Prone, and Side Position Exercises With and Without a Swiss Ball. Sports Health. 2016;8(4):372–9.

Hálásan köszönjük Dr. Takács Mária, Kisrákói Andrea és Kiss Dóra segítségét a mérések kivitelezésében. A kutatást az OTKA 115894 és a BME FIKP-BIO támogatta. Petró Bálintot jelen munka során az Emberi Erőforrások Minisztériuma, Új Nemzeti Kiválóság Program 18-3-I-BME-158 ösztöndíja támogatta.

Dr. Kiss Rita M.
Budapesti Műszaki és Gazdaságtudományi Egyetem, Mechatronika, Optika és Gépészeti Informatika Tanszék
H-1111, Budapest, Bertalan Lajos u. 4-6.
Tel.:(+36)1 463-1738

Prospects in innovative manufacturing technologies of UHMWPE

Ágnes Ureczki, Kitti Keszei

Department of Polymer Engineering, Budapest University of Technology and Economics

ureczkia@pt.bme.hu

DOI: 10.17489/biohun/2019/1/04

Abstract

Due to its properties like high load-bearing capacity, biocompatibility, excellent abrasion resistance, and strength, ultra-high molecular weight polyethylene (UHMWPE) is widely used as a bearing material in industrial applications and in the field of joint prostheses. Currently, UHMWPE is produced by compression molding, ram extrusion, hot isostatic pressing and direct compression molding followed by post-processing techniques, such as milling or machining to finalize the prosthesis geometry and to achieve the final tolerances. With post-processing techniques, we are wasting a high-cost material, energy, and time. In this paper, we collected manufacturing technologies that have the potential to be used for creating parts with one-step production, minimalized material loss, and with a view of providing customized manufacturing capabilities. We compared two technologies: (i) FFF printing and (ii) injection-molding. In addition to the feasibility, we focus on the investigation of mechanical properties. Three tests were performed on the manufactured specimens: hardness measurement, tensile test, and scanning electron microscope (SEM).

Keywords: UHMWPE; prosthetics; injection molding; 3D printing; FFF

Introduction

Owing to its high load-bearing capacity, biocompatibility, outstanding mechanical properties, and excellent abrasion resistance, ultra-high molecular weight polyethylene (UHMWPE) is widely used in the industry and also in medical fields, such as in joint prostheses.[1]

Manufacturing technologies for producing UHMWPE are compression molding, ram extrusion, hot isostatic pressing, and direct compression molding.[1] They use powder resin produced from ethylene gas by polymerization with the use of the Ziegler process.[2] Recently we can also find granules form of the UHMWPE on the market, recommended for injection molding, but it is still hard to process the material as it requires high pressure.[1] Its extremely low melt flow rate (MFR = 0.06 g/10 min) and high melt viscosity make the material difficult to process even in the melting state.[1] Although, most of the powder resin-based manufacturing technologies require post-processing techniques, such as milling to finalize the geometry and to achieve the final tolerances.[1] With these post-processing operations, we are wasting material, energy, and time. This is one of the reasons it is important to turn to alternative techniques. We focused on the FFF technology (Fused Filament Fabrication), a layer-by-layer extrusion technique, and injection molding. FFF

technology is recommended for parts in low volumes and parts with unique, customized complex geometries. In the medical field, such as in temporomandibular joint replacement and total knee joint replacement[3-5] the technique could be a beneficial technology from the production side. In the case of standard-sized parts with medium or high volumes, examining injection molding is recommended, which can be used to create complex geometries cost-effectively and fast. In both technologies, we can build the parts from granule form and create products with material addition.

We aim to explore the FFF processability of the material. Based on a literature review, there are different ways of improvements in the field of additive manufacturing. One is working with the SLS[6] technology, using the powder form of the material, and others working with the FFF[7,8] technology, using the filament form of the material. Although there was no precedent for FFF printing pure UHMWPE successfully due to its difficulties in processing, the possibility of additive usage allows us to optimize processing parameters and product attribute parameters, hence to make the processing technology viable. Panin et al.[9] optimized the plasticizing components ratio of the UHMWPE matrix for keeping its excellent mechanical properties but making it easier to produce by the FFF technology (UHMWPE + 15 wt. % HDPE-g-SMA + 15 wt. % PP). With this material, they could even achieve much better tribological properties (1, 4 times) on the 3D printed parts than on the parts produced from the same material by hot-pressed technology. Based on their studies, they recommend fabricating the material by FFF printing for tribomechanical purposes. In the field of injection molding of the UHMWPE material, we can see that it is challenging to process. Some of the analyzed literatures deal with the elimination of the delamination layers derived from the processing technology,[10] while others deal with the development of the manufacturing technology or additives to make the raw material easier to process.[11] Some researches[12] examine the tribological behavior of injection molded UHMWPE.

In this paper, we examined the novel manufacturing technologies of the material, which can be used for creating beneficial products in the long run. We aim to compare two technologies: FFF technology and injection-molding. In addition to the feasibility, we focus on the investigation of the mechanical properties. Our future perspective is to optimize the technology for the UHMWPE material and check the effects of its mechanical, tribological, and morphological properties. Our first step, presented in this paper, is the examination of the feasibility and the mechanical properties of specimens fabricated by the FFF technology.

Materials and methods

During the preliminary experiments, the L4000 (Lubmer, Mitsui Chemicals) commercial-grade UHMWPE was used. The filament for FFF printing was created by a twin-screw extruder, FFF printing was done on a CraftBot3, dual head FFF printer. The machine settings for sample preparation have been optimized manually and will be detailed in a later section. The injection-molded specimens were fabricated by an Arburg 420 C injection molding machine. Three tests were performed on the manufactured specimens: hardness measurement, tensile test, and scanning electron microscope (SEM). Plates were injection molded first then the specimens were milled out of them. A Roland MDX-540 milling machine was used for milling. We used EN ISO 527 5A test specimens for the examinations. Shore D hardness was determined with a Zwick 3114. The tensile tests were performed on a Zwick Z005

Parameter	Value
Injection temperature of the zones [°C]	225-230-235-240-240
Mold temperature [°C]	40
Holding pressure [MPa]	70
Time for holding pressure [s]	20
Injection rate [cm^3/s]	40

Table 1. Injection molding parameters

universal tensile testing machine. The SEM investigations were performed with a Jeol JSM 6380LA scanning electron microscope.

The injection molding settings were determined, taking into account the recommendations on the raw material datasheet. 80x80x4 mm plates with film gates were injection molded using a two-cavity mold. The test specimens were obtained by milling from the injection molded plates. The milling velocity was 12 mm/s, and the speed was 3000 1/min.

Our experiment focused on finding an FFF parameter configuration that can be used to produce specimens from UHMWPE. The biggest challenge during processing the material was to keep the first layer of the material on the bed. From the originally used kapton film coated bed the material started to shrink out immediately. Therefore, we tried different techniques to ensure the good adhesion. A positive result was obtained with a perforated plate. *Table 2* summarizes the process of keeping the first layers attached to the printing bed. The main problem was the high shrinkage of the material.

Table 3 shows the constant and changed parameters used during the process. We worked with high temperature, high infill densities and

Type of bed	Efficiency	Comment/Illustration
Glass with kapton film	No adhesion	No layers remained on the plate.
Atactic PP liquid (Vestoplast W-1750)	The first layer adhered successfully, but the material came up when additional layers were printed.	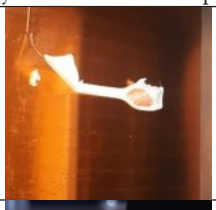
Epoxy-based printed circuit board perforated plate	Feasible. It warmed up but did not soften under the applied temperatures.	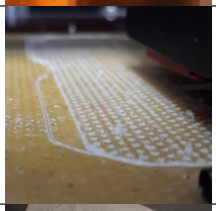
UHMWPE injection molded plate	Proper adhesion, but removal is not feasible from the plate. Furthermore, the plate melted and the extruder head moved on it.	

Table 2. Bed types and their efficiency for keeping the layers on the bed

	Parameter	Value	Optimal value
Constant	Extrusion temperature [C°]	300	-
	Bed temperature [C°]	110	-
	Layer height [mm]	0,2	-
	Infill structure	parallel lines (-45°/45°)	-
	Infill density [%]	100	
Changed	Number of rafts	0-2-5	2
	Infill density of the raft layers [%]	10-50-60-70-80-90-100	100
	Extruded material [%]	100-110	110
	Extrusion speed [mm/s]	10-20	10
	Printing orientation	flat / on-edge	flat
	Use of a dome and door	yes-no	yes

Table 3. FFF printing parameters setup

low printing speed to ensure adequate heating of the material. We also used a dome and a door from Craftbot spare parts to achive an increased temperature of the environment.

The heating and cooling cycles affect the material behaviour and the non-uniform thermal gradients evacuation. Consequently, thermal stresses can accumulate within the part, which can affect the dimensional accuracy and quality (e.g. distortion, warpage) of the printed structure. Thanks to the heated bed, the temperature of the lower layers is higher and the effect of the heated bed during the process is less and less pronounced.[13]

To maximize the physical connection between the specimen and the perforated sheet, we first printed a "raft" under the specimen. This is a larger tray of material printed in few layers before the actual print. In the experiments, printability worked if this "raft" did not consist of more than two layers. *Figure 1* shows the mentioned raft, and also shows that in case of more than two layers of the raft, the material started to shrink out from the perforated plate.

It was advisable to wait until the whole specimen cooled down, otherwise, the printed product would have a greater deformation after the removal from the perforated plate. From the printed parts, we firstly removed the raft layer. It is important to consider that it was impossible to print thin parts, and also, it was also impossible to print complex geometries. *Figure 2* shows that we can only print samples with flat print-

Figure 1. Raft layer evaluation during the process

ing orientation. Although the edges of the specimens are inaccurate in this case, too. The cross-section dimensions are well reproducible, so it can be used for the performed tests.

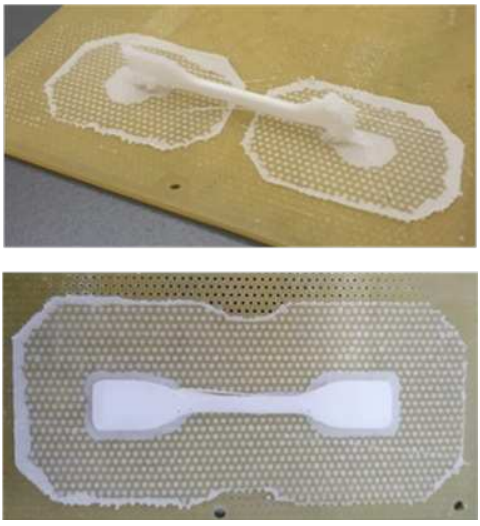

Figure 2. Printed specimens with different orientations

Results

The hardness measurement results show that the fibrous structure of the FFF printed sample influences its hardness. We measured on a surface that appeared to be homogeneously compact. The measured values are given in *Table 4*. Lower shore D value measured on the printed samples. It could be caused by its layer by layer structure. We also measured a higher standard deviation value on the FFF printed samples. The injection-molded samples were more homogenous, all 5 measurements have the same hardness value.

The main parameters used in the tensile test are the following: the clamping distance was 50 mm, the preload was 1 N with 10 mm/min preload speed. The temperature during the measurement was 23.3 °C and the relative humidity was 26.8%. We examined 5-5 specimens of each manufacturing technology and plotted the stress-strain curves of each and their average *(Figure 3)*. *Table 5* shows the characteristic values that can be calculated from the tensile measurement. The curves show different trajectories. The calculated modulus and strength values were lower in the case of the FFF printed than the injection-molded specimens. The different behaviour of the samples can be explained by the orientation of the UHMWPE chains, which is greatly influenced by firstly both filament production and FFF printing and secondly by injection-molding. Elongation at tensile strength is higher in the case of the FFF printed specimens, but elongation at break is significantly lower. It is also important to highlight that there are significant standard deviations mainly in elongation at break in injection-molded parts, which could show that with milling, we probably caused minor surface mistakes on the samples.

During scanning electron microscopy (SEM), we worked at 30-, 100- and 200-fold magnifications. The study aimed to compare the morphological structure of the injection-molded and FFF printed specimens and to investigate the failure characteristics of the FFF printed sample. An accelerating voltage of 10 kV was used. *Figure 4* shows the separation

Sample type	Specimen	Shore D average hardness	Standard deviation
A	L4000, injection molded	63,85	0,34
B	L4000, FFF printed	57,20	0,86

Table 4. Shore D average harnesses

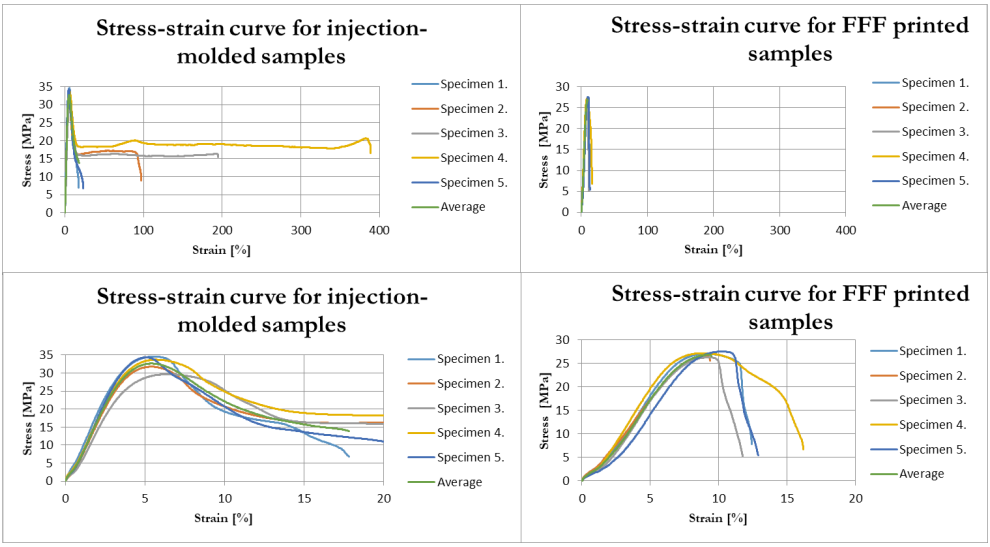

Figure 3. Stress-strain curves

of the first layer from the printed raft in the FFF printed sample, highlighted the air gap between the raft and the first layers. *Figure 5* shows an (I) injection-molded sample broken in liquid nitrogen, (II) an FFF printed sample broken in liquid nitrogen, and (III) an FFF printed sample after the tensile test at 30x 200x magnifications. If we focus on the central areas of the FFF printed pattern (and not on the bottom, base layer), we do not see significant differences. The tensile test results show higher elongation at break in the case of the injection-molded samples. This high elongation could be explained by the formed "skin-core-skin" structure. Because the injection-molded plates are relatively thick, the core structure dominates in their case, where the orientation of the molecules is less significant. In contrast, in the case of the FFF technology, the fibers are highly oriented. This could be one of the reasons for the different elongation behavior of the samples produced by different technologies.

Property	Injection-molding	standard deviation	FFF printing	standard deviation
Tensile strength: σ_M [MPa]	32,80	1,703	26,92	0,405
Elongation at tensile strength: ε_M[%]	5,64	0,426	9,29	0,447
Ultimate tensile strength: σ_B [MPa]	10,95	3,854	10,17	7,092
Elongation at break: ε_B[%]	144,56	126,000	12,54	7,092
Young's modulus: E_h [GPa]	0,68	0,043	0,39	0,045

Table 5. Calculated values from tensile test

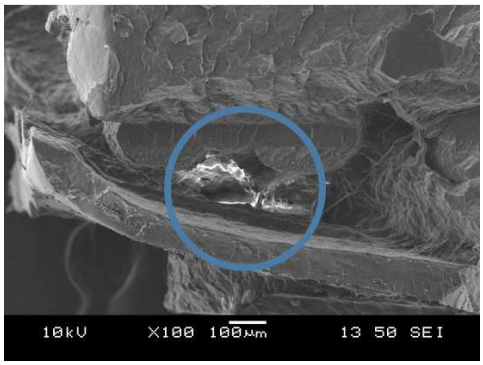

Fig. 4. FFF printed UHMWPE first layer at 100x magnification

It can be also clearly seen from the figure that although the FFF printed samples obtained from the tensile test showed a small elongation at break, the failure of the material is not brittle. For a deeper understanding of the mechanical and morphological properties of the material, further experiments and studies are required.

Discussion

In our research, we investigated the FFF printability of UHMWPE. During our study, we explored the validity of the topic. The favorable mechanical properties of the material and the successful and widely spread use in healthcare, causing the importance of examining new processing technologies. With FFF technology, as the novel method, we can create customized unique geometries. This is one of the reasons why this technology has great importance. In our research, we examined whether it is possible to process the pure UHMWPE material with FFF technology because of the mentioned advantages. During the experiments, it was possible to produce limited specimens made of pure UHMWPE by optimizing the process parameters and using a perforated plate to make physical contact between the UHMWPE layers and the plate.

Still, it was not possible to create complex geometries. Beyond the high processing temperatures, the challenge was the high shrinkage of the material and to ensure good adhesion between the first and base plate layers. The hardness of the test specimens was compared to the samples of the same material

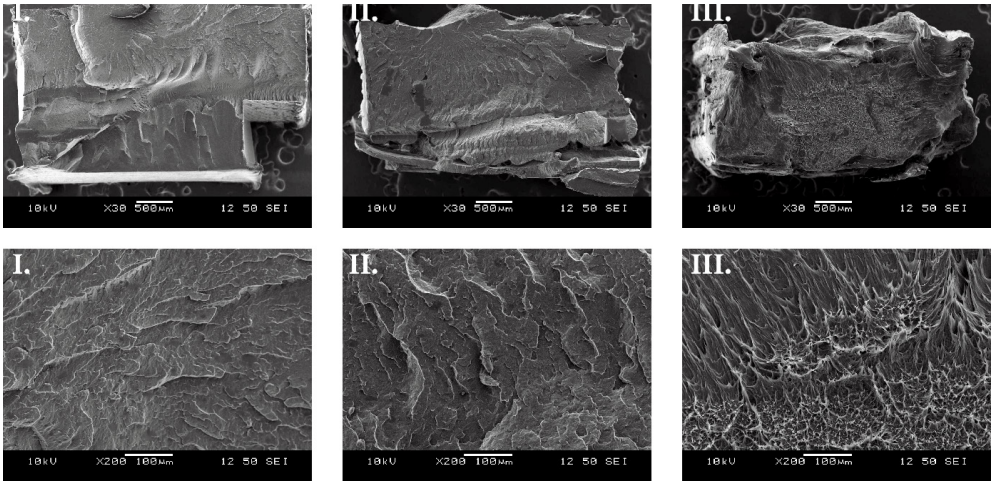

Fig. 5. Injection-molded cryogenic (I.), FFF printed cryogenic (II.) and FFF printed surfaces after tensile test (III.) at 30x and 200x magnifications

made by injection-molding, then tensile test and electron microscopic examination were performed. The FFF printed products showed inferior hardness, lower strength, and modulus than the injection-molded samples. SEM pictures show that the first layer adhesion is a critical part. The filament extrusion and also the FFF printing itself affects the properties of the material and the orientation of the molecular chains. It is important for further examinations to find out how we can minimize shrinkage and create complex products with appropriate dimensional accuracy. Moreover, further measurements are required to verify if the changed material structure and properties are still between favorable limits to allow the usage of FFF printed part in different applications.

REFERENCES

1. *Kurtz SM, editor.* UHMWPE Biomaterials Handbook. 3rd ed. Amsterdam, The Netherlands: Elseiver Inc.; 2016.
2. *Padmanabhan S, Sarma KR, Sharma S.* Synthesis of ultrahigh molecular weight polyethylene using traditional heterogeneous Ziegler-Natta catalyst systems. Industrial & Engineering Chemistry Research 2009;48(10): 4866-4871.
3. *Ackland DC, Robinson D, Redhead M, Lee PVS, Moskaljuk A, Dimitroulis G.* A personalized 3D-printed prosthetic joint replacement for the human temporomandibular joint: From implant design to implantation. Journal of the Mechanical Behaviour of Biomedical Materials 2017;69: 404-411.
4. *De Meurechy N, Braem A, Mommaerts MY.* Biomaterials in temporomandibular joint replacement: current status and future perspectives - a narrative review. International Journal of Oral and Maxillofacial Surgery 2017;47(4): 518-533.
5. *Szojka A, Lalh K, Andrews SHJ, Jomha NM, Osswald M, Adesida AB.* Biomimetic 3D printed scaffolds for meniscus tissue engineering. Bioprinting 2017;8: 1-7.
6. *Rimell JT, Marquis PM.* Selective laser sintering of ultra high molecular weight polyethylene for clinical applications. Journal of Biomedical Materials Research 2000;53(4): 414-420.
7. *Bin Md Ansari MH, Irwan Bin Ibrahim MH.* Thermal characteristic of waste-derived hydroxyapatite (HA) reinforced ultra high molecular weight polyethylene (UHMWPE) composites for fused deposition modelling (FDM) process. Proceeding of Colloquium of Advanced Mechanincs (CAMS2016); 2016 Dec 18-19; Johor, Malaysia. IOP Conference Series: Materials Science and Engineering; 2017.
8. *Panin SV, Buslovich DG, Kornienko LA, Alexenko VO, Dontsov YuV, Shil'ko SV.* Structure, as well as the tribological and mechanical properties, of extrudable polymer-polymeric UHMWPE composites for 3D printing. Journal of friction and wear 2019;40(2): 143–153.
9. *Panin SV, Buslovich DG, Kornienko LA, Alexenko VO, Dontsov YuV, Ovechkin BB.* Structure and tribomechanical properties of extrudable ultra-high molecular weight polyethylene composites fabricated by 3D printing. Proceedings of Oil and Gas Engineering Conference; 2019 Feb 26-28; Omsk, Russian Federation. AIP Conference Proceedings; 2019.
10. *Yilmaz G, Yang H, Turng L.* Injection molding of delamination-free ultra-high-molecular-weight polyethylene. Polymer Engineering & Science 2019;59(11): 1-10.
11. *Xie M, Chen J, Li H.* Morphology and mechanical properties of injection-molded ultrahigh molecular weight polyethylene/polypropylene blends and comparison with compression molding. Journal of Applied Polymer Science 2019;111: 890–898.
12. *Raffi NM, Kanagarajan D, Srinivasan V.* Tribo-

logical behaviour of ultra-high molecular weight polyethylene in a hip joint simulator. Frontiers of Material Science 2012;6(4): 358–365.

13. *Kousiatza C, Chatzidai N, Karalekas D.* Temperature mapping of 3D printed polymer plates: Experimental and numerical study. Sensors 2017;17(3): 456.

Hereby we would like to thank our supervisor Dr. Norbert Krisztián Kovács and my consultant Dr. Gábor Szebényi, who supported the preparation of this paper with the best of their professional knowledge. We would also like to thank the Laboratory Staff of the Department of Polymer Engineering, but especially to Dávid Bartók, György Bartók and István Horváth for their help in preparing the measurements.

The research reported in this paper and carried out at BME was supported by the NRDI Fund (TKP2020 IES, Grant No. BME-IE-BIO) based on the charter of bolster issued by the NRDI Office under the auspices of the Ministry for Innovation and Technology.

The project is funded by the National Research, Development and Innovation (NKFIH) Fund, Project title: „Developing a new generation of customized medical implants and medical aids for additive technologies"; the application ID number: NVKP_16-1-2016-0022. Lubmer L4000 material was supported by Dreyplas GmbH.

Ágnes Ureczki
Budapest University of Technology and Economics, Faculty of Mechanical Engineering, Department of Polymer Engineering
Műegyetem rkp. 3., T. bldg. III., Budapest, Hungary, H-1111
Tel.: (+36) 1 463-3083

Sanatmetal®

Ortopédiai és Traumatológiai Eszközöket Gyártó Kft.

Pannon

csípőprotézis szár család

Világszínvonal,
egyetlen műszerkészlettel!

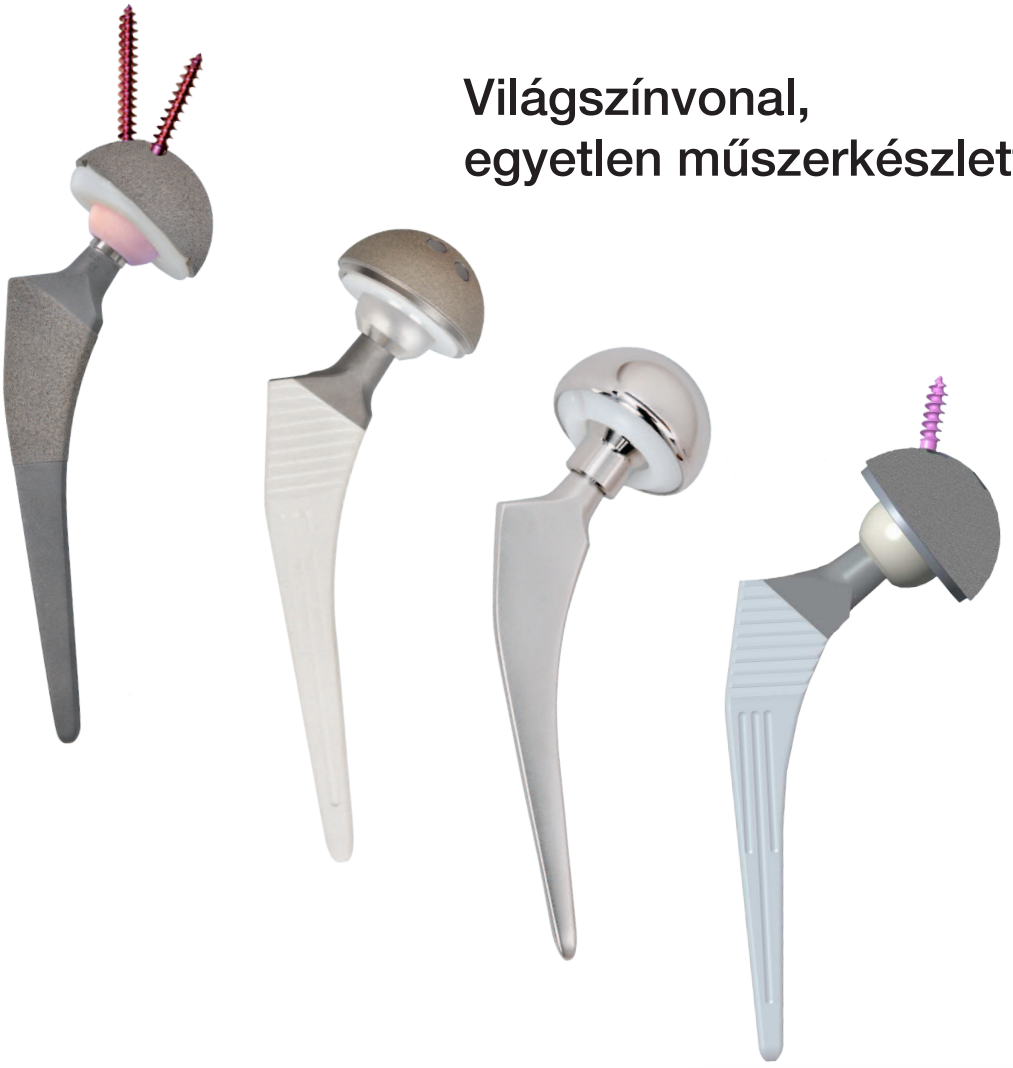

www.sanatmetal.hu

Cím: 3300 Eger, Faiskola út 5.
Telefon: +36 36 512-900
Fax: +36 36 512-932
e-mail: metal@sanatmetal.hu

Tranexamic acid in primary total knee arthroplasty: ideal route of administration

Rakesh K. Gupta, Raj Singh Potalia, Pradyumna Krishna Majumdar, Parth Singh, Avik Neogi

Department of Orthopaedics, PGIMS, Rohtak, Haryana, India

pradyumnakm@gmail.com

DOI: 10.17489/biohun/2019/1/05

Abstract

Background & Study Aims: Consensus is lacking regarding the optimal route and dose of administration of Tranexamic acid (TXA) so this study was conducted to compare the efficacy and safety of topical, oral and intravenous routes (iv) of TXA with routine hemostasis alone in patients undergoing primary total knee arthroplasty (TKA).

Materials and methods: A prospective randomized trial was conducted in patients undergoing primary TKA. Patients were divided into four groups of 50 each; group 1 received intraarticular TXA, group 2 received oral TXA three hours before surgery, group 3 received IV TXA just before tourniquet release and group 4 did not receive TXA. Post-operative drain volume (PODV), fall in haemoglobin (Hb) level and the required amount of blood transfusion were evaluated.

Results: PODV and drop in Hb level respectively were (158 ± 90 ml and 1 ± 0.5 g/dl) in group 1, (328 ± 149 ml and 1.7 ± 0.7 g/dl) in group 2, (311 ± 151 ml and 2.1 ± 1 g/dl) in group 3 and (589 ± 115 ml and 3.2 ± 1.2 g/dl) in group 4. The difference in drain volume between all groups was statistically significant except between groups 2 and 3. Transfusion requirements were significantly greater in group 4 ($p < 0.001$).

Conclusions: Intra-articular, oral and IV TXA were observed to be safe strategies and more effective than tamponade effect alone to reduce drain volume and transfusion requirements after TKA. Additionally, intra-articular TXA was better than oral or IV TXA with respect to drain volume and post-op drop in Hb.

Keywords: total knee arthroplasty; tranexamic acid; intra-articular; oral; intravenous

Introduction

Total knee arthroplasty (TKA) is one of the most commonly performed elective orthopaedic procedures. Wherever indicated, it provides significant pain relief and improvement in the quality of life. Leg swelling, post-operative pain and blood loss are some of the frequent problems following TKA which may compromise the rehabilitation process. Considerable blood loss after TKA is most problematic, requiring significant post-op blood transfusion (BT) which carries a substantial risk of both immunologic reaction and transmission of diseases. Per-operative blood loss is largely restricted during the procedure by the use of a tourniquet. Post-op blood loss accounts for a major component of

total blood loss and most of it occurs during the initial post-op period (24 hours).[1] While the risks of non-transfusion offset those of transfusion-related complications; associated costs, shortage of matched blood products and ineffectiveness of shed autologous blood re-transfusion justify investigating efforts to find new blood conserving methods.[2,3]

Although tranexamic acid (TXA) has been used for over 20 years in surgical practice as an agent to control blood loss on account of its fibrin clot stabilizing property; surgeons have hesitated to use it routinely due to insufficient evidence of its efficacy versus the unresolved issue of possible thromboembolic events.[4,5] It has also been shown to have anti-inflammatory properties that might help in early rehabilitation.[6] The best mode of TXA administration for patients undergoing TKA is not clear.[7] Due to safety concerns with systemic administration of TXA, there has been a growing interest in the intra-articular/ topical use of TXA for curtailing blood loss in orthopaedics. Since intra-articular instillation of TXA can directly target the source of bleeding, it can be considered to be a safer method of delivery while decreasing potential systemic effects, even in hemophilic patients.[8] Other drugs like carbazochrome sodium sulfonate have been used alone or in conjunction with TXA to good effect.[9]

The current study was conducted to determine the best possible route of administration of TXA in patients undergoing TKA to minimize post-op blood loss.

Materials and methods

This study was carried out in our department on two hundred patients after approval from the institutional ethics committee [IEC/Th/17/ Ortho2 (Dated 20/3/17)]. Written informed consent was taken from every patient before surgery. The inclusion criteria were primary osteoarthritis of the knee, no previous surgery in that limb and age group of between 40 to 80 years while the exclusion criteria included bleeding disorder, previous history of adverse drug reaction or allergy to TXA, hepatic, cardio-respiratory or renal insufficiency (serum creatinine >1.5 mg/dl) and recent history of thromboembolic episode.

The patients were divided into four groups of 50 each. Group 1 received 1.5 g intra-articular TXA, Group 2 received 1.95 g of TXA (3 tablets of 650 mg each) with a sip of water three hours before incision, group 3 received 1.5 g IV TXA just before tourniquet release while group 4 did not receive any TXA.

All preoperative medications containing salicylates and NSAID were stopped a week preceding surgery. Pre-operative haematological investigations like Haemoglobin (Hb) and coagulation profile were carried out in all cases.

All surgeries were done under combined spinal-epidural anaesthesia and pneumatic tourniquet. After thorough cleaning and draping, exsanguination of the affected limb was done through elevation for two minutes.

Tourniquet cuff pressure was set to 300 mmHg. A standard medial parapatellar approach with anterior midline incision was used in all the cases. A posterior stabilized cemented knee prosthesis (Stryker, USA) was used in all the patients. No patellar resurfacing was done in any case but was managed by osteophyte removal and cauterization of margins all around the patella. After achieving hemostasis, the wound was closed in layers over a negative suction drain. Tourniquet was deflated after the application of pressure bandage.

In group 1, 1.5 g of TXA diluted in normal saline (NS) to make 50 ml was instilled

	Group 1 (n= 50)	Group 2 (n= 50)	Group 3 (n= 50)	Group 4 (n= 50)
Age	59.2 ± 7	60.7 ± 8.5	59.1 ± 9.2	61.4 ± 8.5
Female	40 (80%)	40 (80%)	36 (72%)	47 (94%)
Male	10 (20%)	10 (20%)	14 (28%)	3 (6%)
Bilateral	2 (4%)	4 (8%)	0	0
Left	22 (44%)	28 (56%)	26 (52%)	22 (44%)
Right	26 (52%)	18 (36%)	24 (48%)	28 (56%)

Table 1. Age, Sex and Side descriptive

through the drain tube while in groups 2, 3 and 4, only 50 ml of NS without TXA was used and the drain was clamped for two hours postoperatively in all patients. The drain was removed after 48 hours of surgery or stoppage of the drain column whichever was later and drain volume was noted. The Hb level at 3rd, 4th and 5th day after surgery was checked and the least of the three values were taken into consideration. Final drain volume and blood transfusions were noted. BT was considered if post-op Hb reduced to ≤ 8.5 g% or drain collection of ≥ 500 ml (possible ongoing loss) in the first 8-10 hours or pre to post-op Hb drop of ≥ 4 g%.[10]

Standard post-op care was provided. Quadriceps strengthening exercises and ankle pumps were started on the same evening. The limb was kept elevated on a pillow. Knee bending exercises were started as and when the patient was comfortable. No chemoprophylaxis for deep vein thrombosis was used.

Post-op assessment was done at 1, 2, 3 and 6 months as per the modified Hospital for Special Surgery Knee Scoring System (HSS).[11] All the patients completed the study period and were finally evaluated at 6 months follow up. Any adverse effect from patient admission to final follow up was noted.

Microsoft Excel (2019) spreadsheet and R software for Windows (version 3.6.1) were used. Quantitative data were presented as mean and standard deviation whereas qualitative data were presented as ratio and proportions. ANOVA test was used for detecting the difference between continuous variables that were normally distributed.

	Group 1	Group 2	Group 3	Group 4	*p-value
Drain volume (ml)	158 ± 90	328 ± 149	311 ± 151	589 ± 115	p <0.001 (All comparison significant, except group 2 vs 3)

Table 2. Drain volume (*Kruskal Wallis Test)

	Group 1	Group 2	Group 3	Group 4
Pre-op Hb (g%)	11.9 ± 1.2	11.7 ± 1.2	12.9 ± 1.3	12.5 ± 0.9
Post-op Hb (g%)	10.9 ± 1.1	10 ± 1	10.8 ± 1.1	9.3 ± 1.5
Decrease in Hb (g%)	1 ± 0.5	1.7 ± 0.7	2.1 ± 1	3.2 ± 1.2

p <0.001 (All comparisons significant except group 2 vs 3) (ANOVA test)

Table 3. Pre-op, post-op and fall in Hb

Kruskal Wallis Test was used to analyze the drain volume. A chi-square test was used to check the association between qualitative variables. The point of statistically significant difference was considered when $p < 0.05$.

Results

All the four groups were comparable in terms of age, gender distribution, body mass index, laterality, other demographic and clinical variables, tourniquet time and duration of surgery ($p > 0.2$). Most of the patients were female. *(Table 1)*

The 48 hours drain volume was significantly lesser in all the TXA groups as compared to the control group ($p < 0.001$). The decrease in drain volume was more significant in group 1 as compared to groups 2 and 3 ($p < 0.001$). *(Table 2)*

The mean fall in Hb was maximum in group 4 and least in group 1. The difference was also significant between group 1 and groups 2 and 3 ($p < 0.001$). *(Table 3)*

The incidence of post-op BT was maximum in group 4. Sixty-two patients required BT of which 45 (73%) patients were from group 4 while 5 patients were from group 1 and 6 patients each from groups 2 and 3 (Table IV). There was no statistical difference between the TXA groups.

The pre-operative functional outcome scores were comparable among all the four groups; however, the post-op functional outcome scores were significant between groups 1, 2 and 3 vs group 4 at 1st and 2nd-month follow-ups. *(Table 5)*

While there was a significant improvement in HSS scores at 1st and 2nd month follow up ($p < 0.005$), it was better in TXA groups as compared to the control group. However, at the time of final evaluation at 6 months, the HSS score was comparable in all the groups.

No. of Blood units transfused	Group 1 (n= 50)	Group 2 (n= 50)	Group 3 (n= 50)	Group 4 (n= 50)
0	45 (90%)	44 (88%)	44 (88%)	5 (10%)
1	4 (8%)	6 (12%)	6 (12%)	28 (56%)
2	1 (2%)	0	0	17 (34%)

Chi-square, p < 0.001, All comparisons significant (<0.001) except group 1 vs 2, 1 vs 3, 2 vs 3 (p > 0.1)

Table 4. Requirement of blood transfusion

Modified HSS score	Group 1	Group 2	Group 3	Group 4
Pre-op	19.4 ± 4.7	20.2 ± 5	18.7 ± 9.3	17.3 ± 4.6
1 month	50.2 ± 1.6	48.8 ± 0.7	51.6 ± 6.8	45 ± 3
2 months	62.0 ± 2.9	62.2 ± 3.5	66.7 ± 8.7	54 ± 3.5
3 months	79.7 ± 4	79.4 ± 6	81.6 ± 5.8	76.6 ± 5.6
6 months	90.2 ± 3.5	91.5 ± 3.3	92.7 ± 4.7	91.6 ± 2.4

Table 5. Modified HSS knee score (ANOVA)

All the patients were followed up for 2 years to ensure they did not develop complications. Three, five, two and six patients respectively in groups 1, 2, 3 & 4 were lost to followup (all after 7 months).

Discussion

Blood loss is a significant factor in peri-op morbidity following TKA. Reducing it, therefore, is an important objective. A variety of measures have been advocated to minimize the peri-op blood loss like the use of tourniquet, intra-op hemostasis, post-op pressure bandage and various medications.

TXA is widely used in many situations, including trauma, to reduce blood loss and prevent consequent morbidity and mortality. In the recent past, TXA has also been a subject matter of research for reducing blood loss in joint replacement surgeries, especially involving hip and knee. As an antifibrinolytic drug, it counteracts the marked local fibrinolysis associated with the release of the tourniquet which is believed to be the reason for reduced blood loss. There is no consensus as yet on a universally acceptable route of administration (intra-articular, oral or IV), dosage or administration schedule.

Therefore, the present study on 200 patients was conducted to identify the most effective regimen of TXA by comparing drain loss, post-op fall in Hb and requirement of blood transfusion (BT) among the three mentioned methods of administration of TXA with a control group (no TXA). To ensure all patients were comparable with respect to drain volume, in group 1, 1.5 g TXA diluted in NS to make (a volume of) 50 ml, was instilled into the knee through the drain while 50 ml NS was instilled in rest of the groups (oral, IV and control) to equate the tamponade effect.

Final drain volume was 158 ± 90 ml, 328 ± 149 ml, 311 ± 151 ml and 589 ± 115 ml in groups 1, 2, 3 and 4 respectively. The difference was significant between all TXA groups and the control group ($p < 0.001$). Moreover, intra-articular TXA was observed to have an advantage over oral and IV TXA routes ($p < 0.001$) in this regard. Similar studies using intra-articular TXA conducted by Aggarwal et al, Ishida et al, Paphon et al, Camerasa et al and Jansen et al observed a mean drain volume of 168 ml, 210 ml, 309 ml, 787 ml and 678 ml respectively.[12–16] The difference in values of Ishida et al and Paphon et al study can be attributed to reduced dosage strength and volume of intra-articular TXA used (200 mg/20 ml NS and 250 mg/20 ml NS respectively as compared to the present study where a dose of 1.5 g/50 ml NS was used).[13-14]

In a similarly sized study, Zhang et al observed that patients injected with intra-articular TXA

as well as peri-articular TXA had a median drain volume of 57 ml. This could be due to the dual injection and longer contact period in their study of 4 hours as well as drain removal after just one day.[17]

Maniar et al reported a larger drain volume of 385 ml in their study on intra-articular TXA, even though TXA was used in a higher dose (3 g/ 100 ml NS) than our study (158 ml, 1.5 g & 50 ml respectively). This may be however due to lesser contact period of the drug in their study (applied locally on the wound surface after cementing the implant and before tourniquet release for a contact period of only 5 minutes).[18]

Sehat et al in their study observed that following TKA only the final drain volume (measured visible blood loss) is usually known and this underestimates the true total loss, as some loss is hidden.[19] To account for hidden blood loss besides what was apparent in drain volume, post-op fall in Hb was also taken into consideration in the present study. It was presumed that blood volume would reach pre-op level by 3rd post-op day, even then, least of post-op Hb level on 3rd, 4th and 5th day was taken to further eliminate any chance of error. The fall in Hb was maximum in group 4 while among TXA groups it was higher in group 2 and 3 as compared to group 1 [3.2 ± 1.2 g%, 1.7 ± 0.7 g%, 2 ± 1 g% and 1 ± 0.5 g% respectively] ($p < 0.001$). As a result, there was a minimal requirement in post-op BT in the TXA groups following TKA. While most of the patients in the control group met the criteria for transfusion trigger thereby resulting in one or more units of BT (45 out of 50 patients), the requirement in TXA groups was negligible (17 out of 150 patients). Out of these few patients requiring post-op BT in TXA groups, almost all of them were on account of either one or two-stage bilateral TKA, or due to the patient having a pre-op Hb of 10 g%. There were no adverse effects in any of the patients despite not giving any DVT chemoprophylaxis.

While there was a significant improvement in HSS scores at follow up ($p < 0.005$), it was better in TXA groups in the initial months as compared to the control group, similar to the findings of Hirose et al, probably due to its anti-inflammatory action.[6,20]

The limitations of our study included a relatively small sample size and no double-blinding in the study. A further possibility of some of the intra-articular TXA getting absorbed into the systemic circulation cannot be ruled out.

Conclusion

The present study confirms the effectiveness of TXA administration by any route (intra-articular/ oral/ IV) in the reduction of postoperative blood loss following primary TKA without any adverse effects. Further, it also indicates that intra-articular TXA in the dosage prescribed is the most effective route of administration as compared to oral or IV administration.

References

1. *Magill P, Cunningham EL, Hill JC, Beverland DE.* Identifying the period of greatest blood loss after lower limb arthroplasty. Arthroplasty Today. 2018;4: 499–504. doi: 10.1016/j.artd.2018.09.002
2. *Bolton-Maggs PHB, Cohen H.* Serious Hazards of Transfusion (SHOT) haemovigilance and progress is improving transfusion safety. Br J Haematol. 2013;163: 303–314. doi: 10.1111/bjh.12547

3. *Miao Y, Guo W, An L, Fang W, Liu Y, Wang X, et al.* Postoperative shed autologous blood reinfusion does not decrease the need for allogeneic blood transfusion in unilateral and bilateral total knee arthroplasty. PLoS ONE. 2019;14. doi: 10.1371/journal.pone.0219406
4. *Panteli M, Papakostidis C, Dahabreh Z, Giannoudis PV.* Topical tranexamic acid in total knee replacement: a systematic review and meta-analysis. The Knee. 2013;20: 300–309. doi: 10.1016/j.knee.2013.05.014
5. *Krivokuca I, Lammers J-WJ.* Recurrent pulmonary embolism associated with a hemostatic drug: tranexamic acid. Clin Appl Thromb Off J Int Acad Clin Appl Thromb. 2011;17: 106–107. doi: 10.1177/1076029609340902
6. *Wu K-T, Siu K-K, Ko J-Y, Chou W-Y, Kuo S-J, Hsu Y-H.* Tranexamic Acid Reduces Total Blood Loss and Inflammatory Response in Computer-Assisted Navigation Total Knee Arthroplasty. BioMed Res Int. 2019;2019. doi: 10.1155/2019/5207517
7. *Larson A, Hoitsma S, Metzger J, Oehlke K, Bebensee S.* Impact of Tranexamic Acid on Blood Loss and Need for Blood Transfusions in Total Knee and Total Hip Arthroplasty. Fed Pract. 2017;34: 14–19.
8. *Huang ZY, Huang Q, Zeng HJ, Ma J, Shen B, Zhou ZK, et al.* Tranexamic acid may benefit patients undergoing total hip/knee arthroplasty because of haemophilia. BMC Musculoskelet Disord. 2019;20. doi: 10.1186/s12891-019-2767-x
9. *Luo Y, Zhao X, Releken Y, Yang Z, Pei F, Kang P.* Hemostatic and Anti-Inflammatory Effects of Carbazochrome Sodium Sulfonate in Patients Undergoing Total Knee Arthroplasty: A Randomized Controlled Trial. J Arthroplasty. 2020;35: 61–68. doi: 10.1016/j.arth.2019.07.045
10. *Nadler SB, Hidalgo JH, Bloch T.* Prediction of blood volume in normal human adults. Surgery. 1962;51: 224–232.
11. *Rosso F, Cottino U, Dettoni F, Bruzzone M, Bonasia DE, Rossi R.* Revision total knee arthroplasty (TKA): mid-term outcomes and bone loss/quality evaluation and treatment. J Orthop Surg. 2019;14. doi: 10.1186/s13018-019-1328-1
12. *Aggarwal AK, Singh N, Sudesh P.* Topical vs Intravenous Tranexamic Acid in Reducing Blood Loss After Bilateral Total Knee Arthroplasty: A Prospective Study. J Arthroplasty. 2016;31: 1442–1448. doi: 10.1016/j.arth.2015.12.033
13. *Ishida K, Tsumura N, Kitagawa A, Hamamura S, Fukuda K, Dogaki Y, et al.* Intra-articular injection of tranexamic acid reduces not only blood loss but also knee joint swelling after total knee arthroplasty. Int Orthop. 2011;35: 1639–1645. doi: 10.1007/s00264-010-1205-3
14. *Sa-ngasoongsong P, Channoom T, Kawinwonggowit V, Woratanarat P, Chanplakorn P, Wibulpolprasert B, et al.* Postoperative blood loss reduction in computer-assisted surgery total knee replacement by low dose intra-articular tranexamic acid injection together with 2-hour clamp drain: a prospective triple-blinded randomized controlled trial. Orthop Rev. 2011;3. doi: 104081/or.2011.e12
15. *Camarasa MA, Ollé G, Serra-Prat M, Martín A, Sánchez M, Ricós P, et al.* Efficacy of aminocaproic, tranexamic acids in the control of bleeding during total knee replacement: a randomized clinical trial. Br J Anaesth. 2006;96: 576–582. doi: 10.1093/bja/ael057
16. *Jansen AJ, Andreica S, Claeys M, D'Haese J, Camu F, Jochmans K.* Use of tranexamic acid for an effective blood conservation strategy after total knee arthroplasty. Br J Anaesth. 1999;83: 596–601. doi: 10.1093/bja/83.4.596
17. *Zhang S, Wang C, Shi L, Xue Q.* Multi-route applications of tranexamic acid to reduce blood loss after total knee arthroplasty: a randomized controlled trial. Medicine (Baltimore). 2019;98. doi: 10.1097/MD.0000000000016570
18. *Maniar RN, Kumar G, Singhi T, Nayak RM, Maniar PR.* Most effective regimen of tranexamic acid in knee arthroplasty: a prospective randomized controlled study in 240 patients. Clin Orthop. 2012;470: 2605–2612. doi: 10.1007/s11999-012-2310-y
19. *Sehat KR, Evans RL, Newman JH.* Hidden blood loss following hip and knee arthroplasty. Correct

management of blood loss should take hidden loss into account. J Bone Joint Surg Br. 2004;86: 561–565.
20. *Hirose H, Ogawa H, Matsumoto K, Akiyama H.* Periarticular injection of tranexamic acid promotes early recovery of the range of knee motion after total knee arthroplasty. J Orthop Surg Hong Kong. 2019;27: 2309499019864693. doi: 10.1177/2309499019864693

Pradyumna K. Majumdar
17/11J, PGIMS Campus
Rohtak, Haryana – 124001
Tel: +91-79881-53640

Does pes planus influence standing balance in elementary school-age children?

Mária Takács[1], Gergely Nagymáté[2], Rita M. Kiss[2]

[1] Department of Orthopedics, MÁV Hospital Szolnok

[2] Department of Mechatronics, Optics and Mechanical Engineering Informatics, Budapest University of Technology and Economics

drtakacskmaria@freemail.hu

DOI: 10.17489/biohun/2019/1/01

Abstract

Purpose: No any research in literature was found to investigate the effect of pes planus on standing balance in school-aged children. Any kind of change in the arches (height, flexibility) may increase the possibility of a change in standing balance. The aim of present study is to determine the influence of pes planus on the standing balance of school-aged children based on independent time-distance and frequency based parameters.

Materials and Methods: Subjects included 177 children (105 neutral and 72 with pes planus). The parameters were determined from the motion of the centre of pressure (COP) on a platform equipped with pressure gauge sensors, on which the subjects were standing for 60 seconds with both feet and open eyes.

Results: When comparing the neutral and pes planus groups, none of the 17 time-distance and frequency based parameters showed any significant difference ($p \geq 0.169$).

Conclusion: The results show that pes planus does not affect significantly standing balance; the differences (however not significant) between the two groups showed a poorer postural control in school-aged children with pes planus. It may be compensated by the increased ML dimension of the base of support.

Keywords: standing balance, center of pressure, children, pes planus, postural control

Introduction

Foot pressure basically determines the quality of our daily activities like working, walking and running, since the leg is responsible for the force which creates the motion and for supporting the human body during standing. Keeping the balance is a dynamic central nervous system controlled process, which could be affected by visual, vestibular and various orthopaedic lesions.[1] According to the definition, standing balance (or static postural control) is the ability to keep the body „motionless" in given circumstances and in a given position, i.e., to stabilize and minimize the movements of the centre of mass (COM).[2] With the help of the inverted pendulum principle it can be proved that during standing the movement of the centre of mass (COM) can be characterized properly by the movement of the foot centre of pressure (COP).[2] During standing, COP excursions are computed from the ground reaction forces, which provide an indication of postural control during quiet standing. From the two-dimensional COP coordinates obtained in the measurement interval numerous COP parameters can be calculated, which can be classified into time-domain and frequency-domain parameters. Despite the fact that the International Society for Posture and

Gait Research has standardised many aspects of static stabilometry measurements in 2009[3] a wide variety of parameters characterizing standing balance are still used by researchers also in the case of children.[4] However, an individual with a high magnitude or velocity of COP excursions is thought to have impaired postural control.[1,4]

Legs, especially the fingers and the metatarsal area, play an important role in keeping the balance, pronated and supinated foot structures change the response time of the muscles around the talo-tibial joint.[5,6] This suggests that any kind of change (height, flexibility) of the arches will also increase the possibility of a change in standing balance. The effect of foot structure change (pes rectus and pes planus) on standing balance is not a widely researched area. The foot structure change effect in the distribution of pressure on the surface of the sole.[6] Pes planus (pronated flat-arched foot) may be associated with excessive subtalar joint pronation. Abnormal compensatory foot pronation may cause passive instability and hypermobility of the joints of the foot.[5] Pes planus may therefore be unstable during weight bearing and might impair standing balance.[7]

When Hertel et al[8] compared young subjects with pes planus foot structures to those with pes rectus foot structures, they did not find any difference between the COP sway area nor between the average COP sway velocity values. At the same time, Cobb et al[7] found significant differences in the pes planus group in case of anterior and posterior deformations during standing position measurements on one leg and with eyes closed (forefoot varus greater than 7°), so they assumed that this group had a poorer postural stability too. In their view,[7] decreased stability associated with increased forefoot varus may be caused by decreased joint congruity and consequently an increased reliance on soft tissue structures for stability. Both studies[7,8] classified the foot structure with a combination of weight bearing and non-weight bearing rearfoot and forefoot measures which caused a great variability in COP area and the average of the standard deviation of the ground reaction forces in both groups. This high variability could lead to opposite conclusions.

Cobb et al[7] were confirmed by the research of Tsai et al[9] and Cote et al[10], because in these research works the values in anterior-posterior and in medial-lateral deformation and in COP sway and average COP sway velocity were significantly higher in the pes planus groups than in the neutral groups. According to Al Abdulwahab and Kahanatchu[11] in case of young adults, pes planus does not affect standing balance since neither in the neutral nor in the pes planus groups were there any significant differences in COP sway velocity and foot pressure index. Sung et al[12] found significant differences in kinetic stability index during single leg stance, if the eyes were closed. In our opinion, the very short measurement times (5-15 seconds) and the standing balance characterized by different parameters could be behind the controversy found in literature. This confirms too, that the sampling time could affect the size of the parameters. A recent study by Scoppa et al[3] suggests short sampling time (25 seconds) for COP summary measures.

However, Carpenter et al[13] recommended 60 seconds long interval time to ensure stable standard deviation of COP parameters for quiet standing trials when vision is available.
No any research in literature was found to investigate the effect of pes planus on standing balance in elementary school-aged children. However, it would be very important because standing balance is constantly evolving, so it changes significantly in childhood.[9] The objective of the present study is to determine

the influence of pes planus on the standing balance of school-aged children during 60-seconds-long bipedal standing with open eyes. The 60 seconds test ensures reliable use of frequency-based parameters. Nagymáté and Kiss[14,15] studied many of time- distance and frequency based parameters with correlation analysis and variance analysis in different standing conditions to select the independent CoP parameters that sensitive enough to show differences between the different standing conditions. The authors of the present research recommended time-distance and frequency parameters as independent CoP parameter sets presented in *Table 1*. Time-distance type parameters characterise the COP movement by its excursions, spatial limits and speed of the motion. The frequency type parameters provide information of the frequency content of the COP motion, which is not trivial by the visual representation of the COP stabilogram, while the effect of the distance type parameters is rather visible. The recommendation of independent parameters is based on correlation and variance analysis of the COP parameters in different stance types and visual conditions. Since the parameters are independent, they can help us analyse the postural control of our subjects in different aspects. We hypothesized that, as in young adults, the standing balance parameters of the pes planus group differ significantly from the neutral group's parameters due to increased passive instability.

Materials and Methods

Subjects

From September 2015 to June 2016, 335 children (192 girls and 143 boys) were screened for the study in three state elementary schools in Region Szolnok (Hungary). The basic inclusion criterion for the subjects was 6-14 years of age. Conditions for exclusion included the following: any minor orthopaedic lesion of the lower limbs, surgery in the past 6 months, lower extremity injury, spine deformity (scoliosis, Scheuermann's disease), bad posture, cerebral palsy, cerebral concussion, visual or vestibular disorder, ±5 dioptres of vision correction, inner ear infection at the time of the examination, upper respiratory infection, or head cold. We also excluded those children who regularly performed exercises which improve balancing ability at high levels (ballet, sailing, tai chi).

In the orthopaedic examination during the first selection, by taking into account the inclusion and exclusion criteria, 12 children (3 girls and 9 boys) were excluded due to minor orthopaedic lesions, surgery, or injuries, 29 children (12 girls and 17 boys) due to scoliosis or Scheuermann's disease, 46 children (24 girls and 22 boys) due to bad posture, 3 boys due to cerebral concussions, visual or vestibular disorders, 2 boys due to ±5 dioptres visual correction and 6 children (2 girls and 4 boys) due to the regular performance of exercises which greatly improve balancing ability.

The research was authorized by the Research Ethics Committee of MÁV Hospital (license number: FI/5-93/2007). The parents of the subjects received detailed verbal and written information in each case before they signed the consent form. The current study conforms to the STROBE statement for reporting of case-control study.[16]

Classification of weight-bearing foot structures

The remaining 237 children (151 girls, 86 boys) were divided into three groups according to their rearfoot-to-leg angles and the medial longitudinal arch angle which determine the foot structure.[9] Tsai et al[9] defined the rearfoot-

Parameter name	Dimension	Description
Time-distance parameters		
Confidence ellipse area (CE area)	mm^2	The area of the 95% confidence ellipse around the CoP trajectory
Confidence ellipse axis ratio (CE axis ratio)	1	The ratio between the major and the minor axes of the 95% confidence ellipse that describes the shape of the CoP's trajectory expansion.
Path length	mm	The length of the total CoP trajectory during the measurement.
Maximum path velocity	mm/s	The filtered maximum distance between consecutive CoP points divided by the sampling interval.
AP-ML range ratio	1	The ratio of the largest CoP path expansions in the anteroposterior (AP) and mediolateral (ML) directions that describes the relation of the largest random errors of postural control between the two anatomical directions.
Anterior (AP+) and Posterior (AP-) maximum deviations	mm	The maximum excursions in the anterior and posterior direction relative to the average CoP point in the AP-ML plane
Largest amplitude during balancing (LA)	mm	The largest continuous motion in both the AP and the ML directions, which are not necessarily equal to the corresponding CoP range. This parameter is similar to the sub-movement size that was defined by[22] for targeted CoP movements.
Frequency parameters		
Frequency power ratios between low-medium and medium-high frequency bands (LMR, MHR)	1	Provide information about the power distribution of postural sway in the frequency domain. The defined limits of the compared frequency bands are low- (0-0.3 Hz) medium- (0.3-1 Hz) and high frequency (1-5 Hz) bands.[23]
Mean power frequency (MPF)	Hz	A weighted average frequency where fj frequency components are weighted by their Pj power. M is the number of frequency bins. MPF is calculated as proposed by Oskoei and Hu 24, according to the following equation: $\boldsymbol{MPF = \sum_{j=1}^{M} f_j P_j / \sum_{j=1}^{M} P_j}$
Spectral power ratio (SPR)	1	The ratio of the total spectral power in the AP direction and the total spectral power in the ML direction. SPR characterizes the rate of power distribution of postural sway frequencies in the AP/ML directions.
Other		
Load distribution difference (LDD)	%	Shows the difference in the weight load on the lower limbs. This parameter is not derived from CoP motion, but it is used by the original Zebris WinPDMS software together with the CoP parameters and proven to be very useful in biomechanical analyses.[25]

Table 1. Studied parameters

to-leg angle as "the acute angle between the bisecting line of the calcaneus and the bisecting line of the distal one third of the leg". They defined the medial longitudinal arch angle as "the obtuse angle between the line connecting the medial malleolus and navicular tuberosity, and the line connecting the navicular tuberosity and the most medial aspect of the first metatarsal head". The children in the neutral foot type group had rearfoot-to-leg angle between 3° and 9° and medial longitudinal arch angle between 134° and 150°.[9] In the pes planus (pronated) foot type group the children had rearfoot-to-leg angle greater than 9° and medial longitudinal arch angles less than 134°.[9] The third foot type group contained children with rearfoot-to-leg angle less than 3° and medial longitudinal arch angles greater than 150°.[9]

Standardization of the effect of a supinated foot structure was not in the scope of the study, therefore 28 children (20 girls, 8 boys) was excluded. Children with asymmetric foot structure (15 girls, 17 boys) were also excluded from the study. No children was found with rigidly pronated feet, which lesion was verified by the method of Tsai et al.[9] In the end, two groups – one with 105 children (84 girls, 21 boys) with neutral foot type and another 72 children (32 girls, 40 boys) with pes planus (pronated, flat arched) foot type – were formed.

Measurement method

Standing balance measurements were carried out with a Zebris FDM-S multifunctional (320 mm x 470 mm measuring surface with 1504 pcs. load cells) (ZEBRIS GmbH, Isny, Germany) at the Biomechanical Laboratory of MÁV Hospital (Szolnok, Hungary). Vertical force distribution data was recorded by the Zebris WinPDMS processing software (v1.2) at 100 Hz.

Each subject performed 60-second trials of barefoot bipedal stance with open eyes in light of day. During these measurements the subjects were in a bipedal natural standing position with a distance between the two ankle joint centres equal to the distance between the right and left anterior superior iliac spines. Both limbs were in full knee extension, heels were aligned in a line, feet were parallel and faced forward and arms were resting by the sides. The subjects focused on a black mark placed approximately 3 m away at eye level on a white wall in front of them. Correct feet placements had to be held throughout the examinations because changes thereof could affect stabilometry parameters.[17] Every subject was asked to perform the required 60-second bipedal standing as motionlessly as possible. Subjects were given 1 practice and 1 test trial, with 1-minute rest periods between the consecutive trials. The trials were accepted only when the subjects maintained the required position for a minimum of 60 consecutive seconds. If they were not able not keep balance, they could repeat the measurements once more. If they could not succeed, they were excluded from the study. The 60 second long measuring ensures the calculation of frequency-type parameters[13] and the difference could be easier detected during the 60 seconds-long bipedal standing with open eyes.

Calculated parameters

Further data processing and COP parameter calculations were carried out on exported raw measurement data in a custom application written in LabVIEW v2013 (National Instruments Inc., Austin, Texas). The calculated instantaneous COP coordinates were filtered with a Butterworth low-pass digital filter with a cut-off frequency of 10 Hz as recommended by Ruhe et al.[18] From the COP position signals, a power spectrum was obtained using the Fast Fourier Transformation (FFT) with Hanning

filtering window as recommended by Ruhe et al.[18] Seventeen time-distance and frequency based parameters were calculated from COP position, which are recommended as indented parameters in,[14,15] summarized in *Table 1*.

Data analysis

To analyse the impact of the pes planus, the average and standard deviation of the selected parameters were calculated for both groups as basic statistical features. Comparison of the two groups was carried out by a Student's t-test confirmed by F-tests to test the homogeneity of variance of the comparable parameters. The level of significance was set to 0.05.

Results

The characteristics of the subjects in the two (neutral and pes planus) foot structure groups are shown in *Table 2*. Anthropometric data (age, height, weight) did not differ significantly, whereas the two parameters describing the foot structure (rearfoot-to-leg angle and medial longitudinal arch angle) differed significantly in the two groups.

All subjects (105) in the neutral group were able to perform the 60-seconds-long bipedal open eyed standing at first time, whereas the test had to be repeated due to loss of balance in the case of 9 out of 75 children of the pes planus group, but nobody was excluded.

The statistics have been performed after excluding 8 outlier from the neutral group and 7 from the pes planus group. The average and standard values of the selected parameters in both groups are shown in *Table 3*. Many parameters show relatively large SD values compared to the mean value, however in most cases they do not differ between the two groups The F-test only shows significant difference in the standard deviations in the ML MHR parameter ($p<0.01$). According to the t-test no parameters show significant differences in the mean between the normal and the pes planus groups. This means that the postural control in the school aged children is not influenced by pes planus.

Discussion

The averages and standard deviations of the 17 independent parameters which characterize the balancing ability of 105 children (84 girls, 21 boys) with a neutral foot type and 72 children (32 girls, 40 boys) with pes planus (pronated, flat arched) are shown in *Table 3*. According to our knowledge, this is the first article about standing balance analysed with distance, time and frequency based parameters calculated from the results of 60-seconds-long

		neutral group N=105 (84 girls, 21 boys)	pes planus (pronated) group N=72 (32 girls, 40 boys)
age (years)		range: 6-14	range: 6-14
weight (kg)		48.5±14.88	48.3±14.59
height (m)		1.53±0.13	1.54±0.10
rearfoot-to-leg angle (deg)	left	5.5±1.6	12.3±1.6
	right	5.6±1.8	11.9±1.7
medial longitudinal arch angle (deg)	left	146.1±1.9	129.1±2.1
	right	145.6±2.1	129.9±2.2

Table 2. Data of the subjects. Values are mean ± SD unless otherwise indicated

measurements at children with neutral and with pes planus foot type. It means, there were no reference values for many examined time-distance and frequency-based parameters,[4] because those parameters were calculated from only 30-seconds-long measurements.[4]

Table 3 shows that many averaged parameters have relatively large SD values. This is due to the intra-subject variability of these COP measures.[19] Papers dealing with the reliability of these parameters reported similarly large relative SD values together with high reliability of the parameters described by Intraclass Correlation Coefficient (ICC).[19] For instance, Laroche et al[19] among many similarly behaving parameter reported 543 mm (95% Confidence interval: 186-900 mm) for COP path length with high reliability of ICC = 0.85. The inter-subject variability of both groups are similar (see F-test values in *Table 2*). In our opinion the higher deviation values compared to the mean values could be caused by the differences in the children's neurological maturity.[20] The parameters of balancing ability vary with age,[20] so the wide range of age (6 to 14 years) of the subjects can cause high SD values. In the neutral group *(Table 2)* the maximum velocity, the 95% CE Area[20] and the path length[21] are in good agreement with the results in young subjects presented in literature.

The aim of the present study was to investigate whether pes planus changes standing balance. By studying the literature, it can be stated that standing balance measurements in children with pes planus foot structure have not been performed yet. We hypothesized that the

	neutral group N=105	pes planus (pronated) group N=72	mean difference	F-test p	t-test p
95% CE axis ratio	1.7 ± 0.571	1.691 ± 0.476	0.010	0.104	0.905
95% CE area (mm2)	262.466 ± 183.086	244.705 ± 186.087	17.761	0.871	0.530
Path length (mm)	855.542 ± 254.855	854.788 ± 222.625	0.754	0.225	0.984
Max velocity (mm/s)	115.359 ± 50.955	117.106 ± 56.328	1.747	0.349	0.830
AP-ML range ratio	1.262 ± 0.486	1.322 ± 0.501	0.060	0.765	0.427
LDD (%)	6.202 ± 5.146	7.19 ± 5.912	0.988	0.196	0.239
AP LA (mm)	28.522 ± 13.076	25.952 ± 10.656	2.570	0.067	0.169
ML LA (mm)	24.577 ± 10.888	23.692 ± 12.023	0.885	0.354	0.611
A max.dev (mm)	26.59 ± 11.072	25.068 ± 11.071	1.522	0.990	0.370
P max.dev (mm)	26.648 ± 11.36	26.723 ± 12.438	0.074	0.396	0.967
AP MPF (Hz)	0.147 ± 0.058	0.155 ± 0.063	0.008	0.446	0.404
ML MPF (Hz)	0.192 ± 0.074	0.191 ± 0.071	0.001	0.661	0.933
SPR	2.005 ± 1.521	2.001 ± 1.762	0.005	0.171	0.985
AP LMR	11.333 ± 9.557	9.868 ± 8.605	1.464	0.347	0.299
AP MHR	11.978 ± 6.308	11.994 ± 7.386	0.017	0.142	0.987
ML LMR	6.79 ± 5.962	5.912 ± 5.144	0.878	0.186	0.311
ML MHR	11.455 ± 4.85	13.297 ± 8.329	1.842	< 0.010	0.094

Table 3. Statistical comparison of the neutral and pes planus groups' standing balance based on COP parameters. Values are mean ± SD unless otherwise indicated.
CE: confidence ellipse, AP: anteroposterior, ML: mediolateral, LDD: load distribution difference between legs, LA: largest amplitude, A: anterior, P: posterior, max dev: maximum deviation, MPF: mean power frequency, SPR: spectral power ratio, LMR: low-medium band power ratio MHR: medium-high frequency band power ratio

children with pes planus foot structures would have had significant poorer standing balance than children with neutral feet, because of reduced stability in the foot joints.[7] Based on the results of 17 independent parameters, the standing balance of children with pes planus is poorer compared to children with neutral feet, however no significant difference was found between the two groups at any parameter ($p \geq 0.169$ *(Table 2)*. It means, our hypothesis could not be justified.

The differences (however not significant) between the two groups *(Table 3)* showed that school-aged children with pes planus could have a poorer postural control, which may be compensated by the increased ML dimension of the base of support coincided with foot pronation. The advantage of increased ML dimension of the base of support is strengthened by the decreased largest amplitude in direction ML (ML LA) and by the decreased mean power frequency in ML direction (ML MPF) in subjects with pes planus compared to neutral group *(Table 3)*. It can be assumed that children's flexible foot structure and increased ML dimension of the base of support are suitable for correction, during the longer measurement time (60 seconds). It means that the different balancing mechanism of young adults has not developed in children yet. The open eyes and bipedal stance could contribute to the compensatory mechanism too. They could be the reason why no significant differences were found in any of the 17 independent parameters.

Controversial results were found comparing standing balance in young adults with pes planus and neutral foot structures. Hertel et al[8] did not find significant differences even in the case of single leg measurements in COP area and COP speed parameters, which was confirmed by the research of Abdulwahab and Kahanatchu.[11] The results are strengthened by the research of Sung et al,[12] because they did not find significant differences in kinetic stability index during single leg stance with open eyes. Cobb et al,[7] Cote et al[10] and Tsai et al[9] found contradictory results, but the features of the standing balance were produced with very short, 5-10-15 second long, one-legged, open and closed eyed measurements.

The limit of study was the fact that the examinations were not performed during single leg stance with open and closed eyes as well as during bipedal stance with closed eyes due to accident prevention considerations.
The present study is unique because the values of the parameters characterizing standing balance were determined according to various criteria in a large number of children with pes planus (79 children) and of neutral foot structures (105 children). Based on the statistical analysis of the results *(Table 3)*, pes planus does not affect significantly standing balance because none of the 17 parameters show any significant difference ($p \geq 0.169$).

The differences (however not significant) between the two groups *(Table 3)* showed that school-aged children with pes planus could have a poorer postural control. Structural changes in the foot did not yet significantly appear in the parameters which describe the balancing ability, however the results of these studies could be highlighted that the pronated foot in elementary school-aged children may be appropriate special clinical improve (special shoe wear, physiotherapy) to improve postural control.

The authors would like to express their gratitude to Ildikó Nagy and to Gábor Szabó physiotherapists for their valuable work in the biomechanical measurements. This work was supported by the Hungarian Scientific Research Fund OTKA [grant number K115894]. The research reported in this paper was supported by the Higher Education Excellence Program of the Ministry of Human Capacities in the frame of Biotechnology research area of Budapest University of Technology and Economics (BME FIKP-BIO)

References

1. *Winter DA, Patla AE, Prince F, Ishac M, Gielo-Perczak K.* Stiffness control of balance in quiet standing. J Neurophysiol. 1998;80(3):1211–21.
2. *Hasan SS, Robin DW, Szurkus DC, Ashmead DH, Peterson SW, Shiavi RG.* Simultaneous measurement of body center of pressure and center of gravity during upright stance. Part II: Amplitude and frequency data. Gait Posture. 1996 Jan 31;4(1):11–20.
3. *Scoppa F, Capra R, Gallamini M, Shiffer R.* Clinical stabilometry standardization. Basic definitions - Acquisition interval - Sampling frequency. Gait Posture. 2013;37(2):290–2.
4. *Verbecque E, Vereeck L, Hallemans A.* Postural sway in children: A literature review. Gait Posture. 2016 Sep;49:402–10.
5. *Franco AH.* Pes Cavus and Pes Planus. Phys Ther. 1987 May 1;67(5):688–94.
6. *Pauk J, Daunoraviciene K, Ihnatouski M, Griskevicius J, Raso J V.* Analysis of the plantar pressure distribution in children with foot deformities. Acta Bioeng Biomech. 2010;12(1):29–34.
7. *Cobb SC, Tis LL, Johnson BF, Higbie EJ.* The effect of forefoot varus on postural stability. J Orthop Sports Phys Ther. 2004;34:79–85.
8. *Hertel J, Gay MR, Denegar CR.* Differences in postural control during single-leg stance among healthy individuals with different foot types. J Athl Train. 2002;37(2):129–32.
9. *Tsai L-C, Yu B, Mercer VS, Gross MT.* Comparison of different structural foot types for measures of standing postural control. J Orthop Sports Phys Ther. 2006;36(12):942–53.
10. *Cote KP, Brunet ME, Gansneder BM, Shultz SJ.* Effects of pronated and supinated foot postures on static and dynamic postural stability. J Athl Train. 2005;40(1):41–6.
11. *Al Abdulwahab SS, Kachanathu SJ.* The effect of various degrees of foot posture on standing balance in a healthy adult population. Somatosens Mot Res. 2015 Jul 3;32(3):172–6.
12. *Sung PS, Zipple JT, Andraka JM, Danial P.* The kinetic and kinematic stability measures in healthy adult subjects with and without flat foot. Foot. 2017;30:21–6.
13. *Carpenter MG, Frank JS, Winter DA, Peysar GW.* Sampling duration effects on centre of pressure summary measures. Gait Posture. 2001 Feb;13(1):35–40.
14. *Nagymáté G, Kiss RM.* Parameter reduction in the frequency analysis of center of pressure in stabilometry. Period Polytech Mech Eng. 2016;60(4):238–46.
15. *Nagymáté G, Kiss RM.* Replacing Redundant Stabilometry Parameters with Ratio and Maximum Deviation Parameters. In: Proceedings of the 12th IASTED International Conference on Biomedical Engineering. Calgary,AB,Canada: ACTAPRESS; 2016. p. 140–4.
16. *von Elm E, Altman DG, Egger M, Pocock SJ, Gøtzsche PC, Vandenbroucke JP.* The Strengthening the Reporting of Observational Studies in Epidemiology (STROBE) Statement: Guidelines for reporting observational studies. Prev Med (Baltim). 2007 Oct;45(4):247–51.
17. *Chiari L, Rocchi L, Cappello A.* Stabilometric parameters are affected by anthropometry and foot placement. Clin Biomech. 2002 Nov;17(9–10):666–77.
18. *Ruhe A, Fejer RR, Walker B.* The test-retest reli-

ability of centre of pressure measures in bipedal static task conditions - A systematic review of the literature. Gait Posture. 2010;32(4):436–45.

19. *Laroche D, Kubicki A, Stapley PJ, Gremeaux V, Mazalovic K, Maillefert JF, et al.* Test-retest reliability and responsiveness of centre of pressure measurements in patients with hip osteoarthritis. Osteoarthr Cartil. 2015;23(8):1357–66.
20. *Hsu YS, Kuan CC, Young YH.* Assessing the development of balance function in children using stabilometry. Int J Pediatr Otorhinolaryngol. 2009;73(5):737–40.
21. *Sakaguchi M, Taguchi K, Miyashita Y, Katsuno S.* Changes with aging in head and center of foot pressure sway in children. Int J Pediatr Otorhinolaryngol. 1994 Apr;29(2):101–9.
22. *Hernandez ME, Ashton-Miller JA, Alexander NB.* Age-related changes in speed and accuracy during rapid targeted center of pressure movements near the posterior limit of the base of support. Clin Biomech. 2012;27(9):910–6.
23. *Nagy E, Toth K, Janositz G, Kovacs G, Feher-Kiss A, Angyan L, et al.* Postural control in athletes participating in an ironman triathlon. Eur J Appl Physiol. 2004;92(4–5):407–13.
24. *Oskoei MA, Hu H.* Support vector machine-based classification scheme for myoelectric control applied to upper limb. IEEE Trans Biomed Eng. 2008 Aug;55(8):1956–65.
25. *Duffell LD, Gulati V, Southgate DFL, McGregor AH.* Measuring body weight distribution during sit-to-stand in patients with early knee osteoarthritis. Gait Posture. 2013 Sep;38(4):745–50.

Mária Takács
Department of Orthopedics, MÁV Hospital Szolnok
H-5000, Szolnok, Verseghy F. str. 6-8,
Tel.: (+36) 56 524 633